14

Molecular spectroscopy 2: electronic transitions

Simple analytical expressions for the electronic energy levels of molecules cannot be given, so this chapter concentrates on the qualitative features of electronic transitions. A common theme throughout the chapter is that electronic transitions occur within a stationary nuclear framework. We pay particular attention to spontaneous radiative decay processes, which include fluorescence and phosphorescence. A specially important example of stimulated radiative decay is that responsible for the action of lasers, and we see how this stimulated emission may be achieved and employed.

The energies needed to change the electron distributions of molecules are of the order of several electronvolts (1 eV is equivalent to about 8000 cm^{-1} or 100 kJ mol^{-1}). Consequently, the photons emitted or absorbed when such changes occur lie in the visible and ultraviolet regions of the spectrum (Table 14.1).

One of the revolutions that has occurred in physical chemistry in recent years is the application of lasers to spectroscopy and kinetics. Lasers have brought unprecedented precision to spectroscopy, made Raman spectroscopy a widely useful technique, and have made it possible to study chemical reactions on a femtosecond time scale. We shall see the principles of their action in this chapter and their applications throughout the rest of the book.

The characteristics of electronic transitions

In the ground state of a molecule the nuclei are at equilibrium in the sense that they experience no net force from the electrons and other nuclei in the molecule. Immediately after an electronic transition they are subjected to different forces and

Synoptic table 14.1* Colour, frequency, and energy of light

Colour	λ/nm	ν/(10^{14} Hz)	E/(kJ mol^{-1})
Infrared	>1000	<3.0	<120
Red	700	4.3	170
Yellow	580	5.2	210
Blue	470	6.4	250
Ultraviolet	<300	>10	>400

* More values are given in the *Data section.*

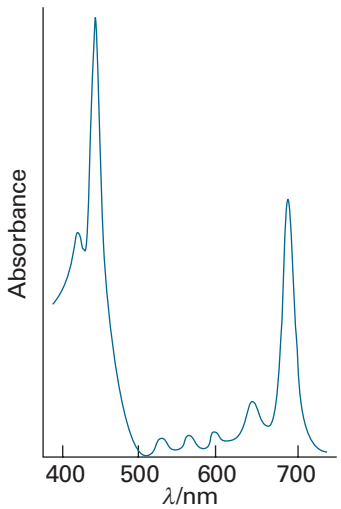

Fig. 14.1 The absorption spectrum of chlorophyll in the visible region. Note that it absorbs in the red and blue regions, and that green light is not absorbed.

the molecule may respond by starting to vibrate. The resulting vibrational structure of electronic transitions can be resolved for gaseous samples, but in a liquid or solid the lines usually merge together and result in a broad, almost featureless band (Fig. 14.1). Superimposed on the vibrational transitions that accompany the electronic transition of a molecule in the gas phase is an additional branch structure that arises from rotational transitions. The electronic spectra of gaseous samples are therefore very complicated but rich in information.

14.1 The electronic spectra of diatomic molecules

We examine some general features of electronic transitions by using diatomic molecules as examples. We begin by assigning term symbols to ground and excited electronic states. Then we use the symmetry designations to formulate selection rules. Finally, we examine the origin of vibrational structure in electronic spectra.

(a) Term symbols

The term symbols of linear molecules (the analogues of the symbols ^{2}P, etc. for atoms) are constructed in a similar way to those for atoms, but now we must pay attention to the component of total orbital angular momentum about the internuclear axis, $\Lambda\hbar$. The value of $|\Lambda|$ is denoted by the symbols Σ, Π, Δ, . . . for $|\Lambda| = 0, 1, 2 \ldots$, respectively. These labels are the analogues of S, P, D, . . . for atoms. The value of Λ is the sum of the values of λ, the quantum number for the component $\lambda\hbar$ of orbital angular momentum of an individual electron around the internuclear axis. A single electron in a σ orbital has $\lambda = 0$: the orbital is cylindrically symmetrical and has no angular nodes when viewed along the internuclear axis. Therefore, if that is the only electron present, $\Lambda = 0$. The term symbol for H_2^+ is therefore Σ.

As in atoms, we use a superscript with the value of $2S + 1$ to denote the multiplicity of the term. The component of total spin angular momentum about the internuclear axis is denoted Σ, where $\Sigma = S, S - 1, S - 2, \ldots, -S$. For H_2^+, because there is only one electron, $S = s = \frac{1}{2}$ ($\Sigma = \pm\frac{1}{2}$) and the term symbol is $^2\Sigma$, a doublet term. The overall parity of the term is added as a right subscript. For H_2^+, the parity of the only occupied orbital is g (Section 11.3c), so the term itself is also g, and in full dress is $^2\Sigma_g$. If there are several electrons, the overall parity is calculated by using

$$g \times g = g \qquad u \times u = g \qquad u \times g = u \tag{14.1}$$

These rules are generated by interpreting g as +1 and u as −1. The term symbol for the ground state of any closed-shell homonuclear diatomic molecule is $^1\Sigma_g$ because the spin is zero (a singlet term in which all electrons paired), there is no orbital angular momentum from a closed shell, and the overall parity is g.

A π electron in a diatomic molecule has one unit of orbital angular momentum about the internuclear axis ($\lambda = \pm 1$), and if it is the only electron outside a closed shell, gives rise to a Π term. If there are two π electrons (as in the ground state of O_2, with configuration $1\pi_u^4 1\pi_g^2$) then the term symbol may be either Σ (if the electrons are travelling in opposite directions, which is the case if they occupy different π orbitals, one with $\lambda = +1$ and the other with $\lambda = -1$) or Δ (if they are travelling in the same direction, which is the case if they occupy the same π orbital, both $\lambda = +1$, for instance). For O_2, the two π electrons occupy different orbitals with parallel spins (a triplet term), so the ground term is $^3\Sigma$. The overall parity of the molecule is

$$(\text{closed shell}) \times g \times g = g$$

The term symbol is therefore $^3\Sigma_g$.

Comment 14.1
It is important to distinguish between the (upright) term symbol Σ and the (sloping) quantum number Σ.

Table 14.2 Properties of O_2 in its lower electronic states*

Configuration†	Term	Relative energy/cm^{-1}	$\tilde{\nu}$/cm^{-1}	R_e/pm
$\pi_u^2\pi_u^2\pi_g^1\pi_g^1$	$^3\Sigma_g^-$	0	1580	120.74
$\pi_u^2\pi_u^2\pi_g^2\pi_g^0$	$^1\Delta_g$	7 882.39	1509	121.55
$\pi_u^2\pi_u^2\pi_g^1\pi_g^1$	$^1\Sigma_g^+$	13 120.9	1433	122.68
$\pi_u^2\pi_u^1\pi_g^2\pi_g^1$	$^3\Sigma_u^+$	35 713	819	142
$\pi_u^2\pi_u^1\pi_g^2\pi_g^1$	$^3\Sigma_u^-$	49 363	700	160

* Adapted from G. Herzberg, *Spectra of diatomic molecules*, Van Nostrand, New York (1950) and D.C. Harris and M.D. Bertolucci, *Symmetry and spectroscopy: an introduction to vibrational and electronic spectroscopy*, Dover, New York (1989).

† The configuration $\pi_u^2\pi_u^1\pi_g^2\pi_g^1$ should also give rise to a $^3\Delta_u$ term, but electronic transitions to or from this state have not been observed.

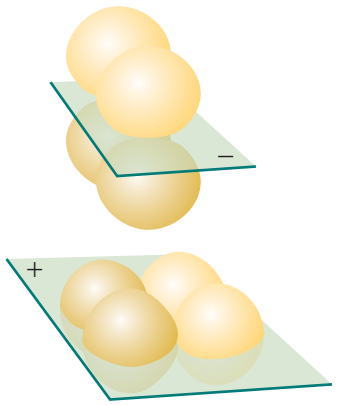

Fig. 14.2 The + or – on a term symbol refers to the overall symmetry of a configuration under reflection in a plane containing the two nuclei.

For Σ terms, a ± superscript denotes the behaviour of the molecular wavefunction under reflection in a plane containing the nuclei (Fig. 14.2). If, for convenience, we think of O_2 as having one electron in $1\pi_{g,x}$, which changes sign under reflection in the *yz*-plane, and the other electron in $1\pi_{g,y}$, which does not change sign under reflection in the same plane, then the overall reflection symmetry is

$$(\text{closed shell}) \times (+) \times (-) = (-)$$

and the full term symbol of the ground electronic state of O_2 is $^3\Sigma_g^-$.

The term symbols of excited electronic states are constructed in a similar way. For example, the term symbol for the excited state of O_2 formed by placing two electrons in a $1\pi_{g,x}$ (or in a $1\pi_{g,y}$) orbital is $^1\Delta_g$ because $|\Lambda| = 2$ (two electrons in the same π orbital), the spin is zero (all electrons are paired), and the overall parity is (closed shell) × g × g = g. Table 14.2 and Fig. 14.3 summarize the configurations, term symbols, and energies of the ground and some excited states of O_2.

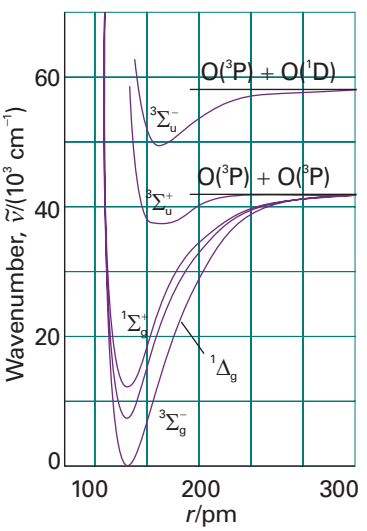

Fig. 14.3 The electronic states of dioxygen.

(b) Selection rules

A number of selection rules govern which transitions will be observed in the electronic spectrum of a molecule. The selection rules concerned with changes in angular momentum are

$$\Delta\Lambda = 0, \pm 1 \qquad \Delta S = 0 \qquad \Delta\Sigma = 0 \qquad \Delta\Omega = 0, \pm 1$$

where $\Omega = \Lambda + \Sigma$ is the quantum number for the component of total angular momentum (orbital and spin) around the internuclear axis (Fig. 14.4). As in atoms (Section 10.9), the origins of these rules are conservation of angular momentum during a transition and the fact that a photon has a spin of 1.

There are two selection rules concerned with changes in symmetry. First, for Σ terms, only $\Sigma^+ \leftrightarrow \Sigma^+$ and $\Sigma^- \leftrightarrow \Sigma^-$ transitions are allowed. Second, the **Laporte selection rule** for centrosymmetric molecules (those with a centre of inversion) and atoms states that:

> The only allowed transitions are transitions that are accompanied by a change of parity.

That is, u → g and g → u transitions are allowed, but g → g and u → u transitions are forbidden.

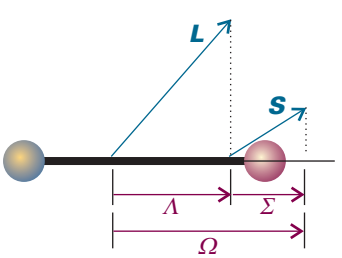

Fig. 14.4 The coupling of spin and orbital angular momenta in a linear molecule: only the components along the internuclear axis are conserved.

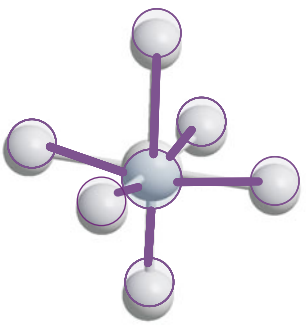

Fig. 14.5 A *d–d* transition is parity-forbidden because it corresponds to a g–g transition. However, a vibration of the molecule can destroy the inversion symmetry of the molecule and the g,u classification no longer applies. The removal of the centre of symmetry gives rise to a vibronically allowed transition.

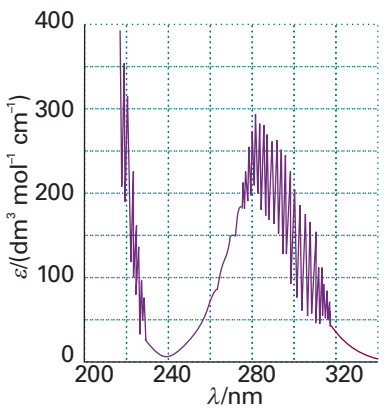

Fig. 14.6 The electronic spectra of some molecules show significant vibrational structure. Shown here is the ultraviolet spectrum of gaseous SO_2 at 298 K. As explained in the text, the sharp lines in this spectrum are due to transitions from a lower electronic state to different vibrational levels of a higher electronic state.

Justification 14.1 *The Laporte selection rule*

The last two selection rules result from the fact that the electric-dipole transition moment

$$\boldsymbol{\mu}_{\mathrm{fi}} = \int \psi_{\mathrm{f}}^{*} \hat{\mu} \psi_{\mathrm{i}} \, \mathrm{d}\tau$$

vanishes unless the integrand is invariant under all symmetry operations of the molecule. The three components of the dipole moment operator transform like x, y, and z, and are all u. Therefore, for a g → g transition, the overall parity of the transition dipole moment is g × u × g = u, so it must be zero. Likewise, for a u → u transition, the overall parity is u × u × u = u, so the transition dipole moment must also vanish. Hence, transitions without a change of parity are forbidden. The z-component of the dipole moment operator, the only component of $\boldsymbol{\mu}$ responsible for $\Sigma \leftrightarrow \Sigma$ transitions, has (+) symmetry. Therefore, for a (+) ↔ (−) transition, the overall symmetry of the transition dipole moment is (+) × (+) × (−) = (−), so it must be zero. Therefore, for Σ terms, $\Sigma^{+} \leftrightarrow \Sigma^{-}$ transitions are not allowed.

A forbidden g → g transition can become allowed if the centre of symmetry is eliminated by an asymmetrical vibration, such as the one shown in Fig. 14.5. When the centre of symmetry is lost, g → g and u → u transitions are no longer parity-forbidden and become weakly allowed. A transition that derives its intensity from an asymmetrical vibration of a molecule is called a **vibronic transition**.

Self-test 14.1 Which of the following electronic transitions are allowed in O_2: ${}^3\Sigma_g^- \leftrightarrow {}^1\Delta_g$, ${}^3\Sigma_g^- \leftrightarrow {}^1\Sigma_g^+$, ${}^3\Sigma_g^- \leftrightarrow {}^3\Delta_u$, ${}^3\Sigma_g^- \leftrightarrow {}^3\Sigma_u^+$, ${}^3\Sigma_g^- \leftrightarrow {}^3\Sigma_u^-$? [${}^3\Sigma_g^- \leftrightarrow {}^3\Sigma_u^-$]

(c) Vibrational structure

To account for the vibrational structure in electronic spectra of molecules (Fig. 14.6), we apply the **Franck–Condon principle**:

> Because the nuclei are so much more massive than the electrons, an electronic transition takes place very much faster than the nuclei can respond.

As a result of the transition, electron density is rapidly built up in new regions of the molecule and removed from others. The initially stationary nuclei suddenly experience a new force field, to which they respond by beginning to vibrate and (in classical terms) swing backwards and forwards from their original separation (which was maintained during the rapid electronic excitation). The stationary equilibrium separation of the nuclei in the initial electronic state therefore becomes a stationary turning point in the final electronic state (Fig. 14.7).

The quantum mechanical version of the Franck–Condon principle refines this picture. Before the absorption, the molecule is in the lowest vibrational state of its lowest electronic state (Fig. 14.8); the most probable location of the nuclei is at their equilibrium separation, R_e. The electronic transition is most likely to take place when the nuclei have this separation. When the transition occurs, the molecule is excited to the state represented by the upper curve. According to the Franck–Condon principle, the nuclear framework remains constant during this excitation, so we may imagine the transition as being up the vertical line in Fig. 14.7. The vertical line is the origin of the expression **vertical transition**, which is used to denote an electronic transition that occurs without change of nuclear geometry.

The vertical transition cuts through several vibrational levels of the upper electronic state. The level marked * is the one in which the nuclei are most probably at

the same initial separation R_e (because the vibrational wavefunction has maximum amplitude there), so this vibrational state is the most probable state for the termination of the transition. However, it is not the only accessible vibrational state because several nearby states have an appreciable probability of the nuclei being at the separation R_e. Therefore, transitions occur to all the vibrational states in this region, but most intensely to the state with a vibrational wavefunction that peaks most strongly near R_e.

The vibrational structure of the spectrum depends on the relative horizontal position of the two potential energy curves, and a long **vibrational progression**, a lot of vibrational structure, is stimulated if the upper potential energy curve is appreciably displaced horizontally from the lower. The upper curve is usually displaced to greater equilibrium bond lengths because electronically excited states usually have more antibonding character than electronic ground states.

The separation of the vibrational lines of an electronic absorption spectrum depends on the vibrational energies of the *upper* electronic state. Hence, electronic absorption spectra may be used to assess the force fields and dissociation energies of electronically excited molecules (for example, by using a Birge–Sponer plot, as in Problem 14.2).

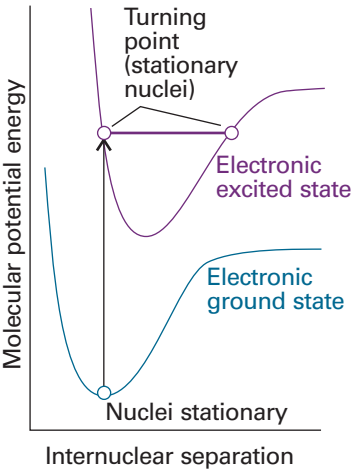

Fig. 14.7 According to the Franck–Condon principle, the most intense vibronic transition is from the ground vibrational state to the vibrational state lying vertically above it. Transitions to other vibrational levels also occur, but with lower intensity.

(d) Franck–Condon factors

The quantitative form of the Franck–Condon principle is derived from the expression for the transition dipole moment, $\boldsymbol{\mu}_{fi} = \langle f|\boldsymbol{\mu}|i\rangle$. The dipole moment operator is a sum over all nuclei and electrons in the molecule:

$$\hat{\boldsymbol{\mu}} = -e\sum_i \boldsymbol{r}_i + e\sum_I Z_I \boldsymbol{R}_I \tag{14.2}$$

where the vectors are the distances from the centre of charge of the molecule. The intensity of the transition is proportional to the square modulus, $|\boldsymbol{\mu}_{fi}|^2$, of the magnitude of the transition dipole moment (eqn 9.70), and we show in the *Justification* below that this intensity is proportional to the square modulus of the overlap integral, $S(v_f,v_i)$, between the vibrational states of the initial and final electronic states. This overlap integral is a measure of the match between the vibrational wavefunctions in the upper and lower electronic states: $S = 1$ for a perfect match and $S = 0$ when there is no similarity.

Justification 14.2 *The Franck–Condon approximation*

The overall state of the molecule consists of an electronic part, $|\varepsilon\rangle$, and a vibrational part, $|v\rangle$. Therefore, within the Born–Oppenheimer approximation, the transition dipole moment factorizes as follows:

$$\begin{aligned}\boldsymbol{\mu}_{fi} &= \langle \varepsilon_f v_f|\{-e\sum_i \boldsymbol{r}_i + e\sum_I Z_I \boldsymbol{R}_I\}|\varepsilon_i v_i\rangle \\ &= -e\sum_i \langle \varepsilon_f|\boldsymbol{r}_i|\varepsilon_i\rangle\langle v_f|v_i\rangle + e\sum_i Z_i\langle \varepsilon_f|\varepsilon_i\rangle\langle v_f|\boldsymbol{R}_I|v_i\rangle\end{aligned}$$

The second term on the right of the second row is zero, because $\langle \varepsilon_f|\varepsilon_i\rangle = 0$ for two different electronic states (they are orthogonal). Therefore,

$$\boldsymbol{\mu}_{fi} = -e\sum_i \langle \varepsilon_f|\boldsymbol{r}_i|\varepsilon_i\rangle\langle v_f|v_i\rangle = \boldsymbol{\mu}_{\varepsilon_f,\varepsilon_i} S(v_f,v_i) \tag{14.3}$$

where

$$\boldsymbol{\mu}_{\varepsilon_f,\varepsilon_i} = -e\sum_i \langle \varepsilon_f|\boldsymbol{r}_i|\varepsilon_i\rangle \quad S(v_f,v_i) = \langle v_f|v_i\rangle \tag{14.4}$$

The matrix element $\boldsymbol{\mu}_{\varepsilon_f,\varepsilon_i}$ is the electric-dipole transition moment arising from the redistribution of electrons (and a measure of the 'kick' this redistribution gives to the electromagnetic field, and vice versa for absorption). The factor $S(v_f,v_i)$, is the overlap integral between the vibrational state $|v_i\rangle$ in the initial electronic state of the molecule, and the vibrational state $|v_f\rangle$ in the final electronic state of the molecule.

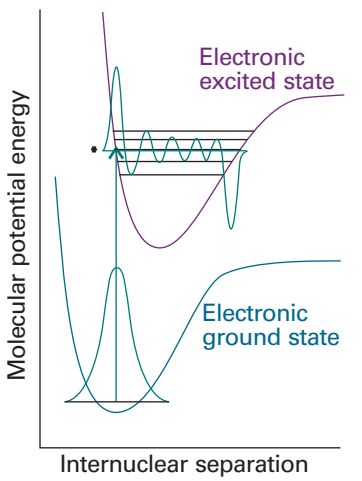

Fig. 14.8 In the quantum mechanical version of the Franck–Condon principle, the molecule undergoes a transition to the upper vibrational state that most closely resembles the vibrational wavefunction of the vibrational ground state of the lower electronic state. The two wavefunctions shown here have the greatest overlap integral of all the vibrational states of the upper electronic state and hence are most closely similar.

Because the transition intensity is proportional to the square of the magnitude of the transition dipole moment, the intensity of an absorption is proportional to $|S(v_f,v_i)|^2$, which is known as the **Franck–Condon factor** for the transition. It follows that, the greater the overlap of the vibrational state wavefunction in the upper electronic state with the vibrational wavefunction in the lower electronic state, the greater the absorption intensity of that particular simultaneous electronic and vibrational transition. This conclusion is the basis of the illustration in Fig. 14.8, where we see that the vibrational wavefunction of the ground state has the greatest overlap with the vibrational states that have peaks at similar bond lengths in the upper electronic state.

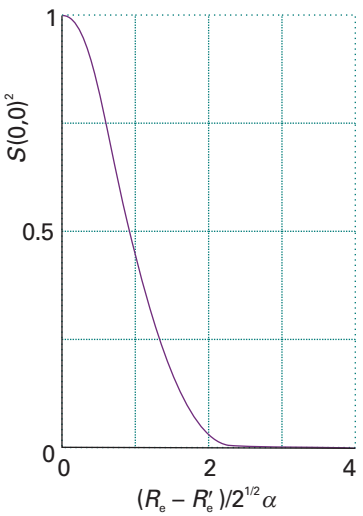

Fig. 14.9 The Franck–Condon factor for the arrangement discussed in Example 14.1.

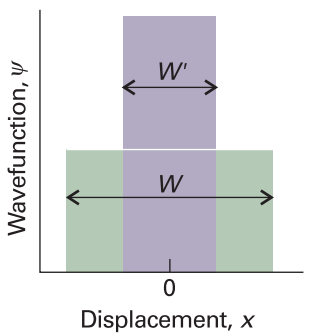

Fig. 14.10 The model wavefunctions used in Self-test 14.2.

Example 14.1 *Calculating a Franck–Condon factor*

Consider the transition from one electronic state to another, their bond lengths being R_e and R'_e and their force constants equal. Calculate the Franck–Condon factor for the 0–0 transition and show that the transition is most intense when the bond lengths are equal.

Method We need to calculate $S(0,0)$, the overlap integral of the two ground-state vibrational wavefunctions, and then take its square. The difference between harmonic and anharmonic vibrational wavefunctions is negligible for $v = 0$, so harmonic oscillator wavefunctions can be used (Table 9.1).

Answer We use the (real) wavefunctions

$$\psi_0 = \left(\frac{1}{\alpha\pi^{1/2}}\right)^{1/2} e^{-x^2/2\alpha^2} \qquad \psi'_0 = \left(\frac{1}{\alpha\pi^{1/2}}\right)^{1/2} e^{-x'^2/2\alpha^2}$$

where $x = R - R_e$ and $x' = R - R'_e$, with $\alpha = (\hbar^2/mk)^{1/4}$ (Section 9.5a). The overlap integral is

$$S(0,0) = \langle 0|0\rangle = \int_{-\infty}^{\infty} \psi'_0\psi_0 dR = \frac{1}{\alpha\pi^{1/2}} \int_{-\infty}^{\infty} e^{-(x^2+x'^2)/2\alpha^2} dx$$

We now write $\alpha z = R - \frac{1}{2}(R_e + R'_e)$, and manipulate this expression into

$$S(0,0) = \frac{1}{\pi^{1/2}} e^{-(R_e-R'_e)^2/4\alpha^2} \int_{-\infty}^{\infty} e^{-z^2} dz$$

The value of the integral is $\pi^{1/2}$. Therefore, the overlap integral is

$$S(0,0) = e^{-(R_e-R'_e)^2/4\alpha^2}$$

and the Franck–Condon factor is

$$S(0,0)^2 = e^{-(R_e-R'_e)^2/2\alpha^2}$$

This factor is equal to 1 when $R'_e = R_e$ and decreases as the equilibrium bond lengths diverge from each other (Fig. 14.9).

For Br_2, $R_e = 228$ pm and there is an upper state with $R'_e = 266$ pm. Taking the vibrational wavenumber as 250 cm^{-1} gives $S(0,0)^2 = 5.1 \times 10^{-10}$, so the intensity of the 0–0 transition is only 5.1×10^{-10} what it would have been if the potential curves had been directly above each other.

Self-test 14.2 Suppose the vibrational wavefunctions can be approximated by rectangular functions of width W and W', centred on the equilibrium bond lengths (Fig. 14.10). Find the corresponding Franck–Condon factors when the centres are coincident and $W' < W$. [$S^2 = W'/W$]

(e) Rotational structure

Just as in vibrational spectroscopy, where a vibrational transition is accompanied by rotational excitation, so rotational transitions accompany the excitation of the vibrational excitation that accompanies electronic excitation. We therefore see P, Q, and R branches for each vibrational transition, and the electronic transition has a very rich structure. However, the principal difference is that electronic excitation can result in much larger changes in bond length than vibrational excitation causes alone, and the rotational branches have a more complex structure than in vibration–rotation spectra.

We suppose that the rotational constants of the electronic ground and excited states are B and B', respectively. The rotational energy levels of the initial and final states are

$$E(J) = hcBJ(J+1) \qquad E(J') = hcB'J'(J'+1)$$

and the rotational transitions occur at the following positions relative to the vibrational transition of wavenumber $\tilde{\nu}$ that they accompany:

$$\text{P branch } (\Delta J = -1): \quad \tilde{\nu}_P(J) = \tilde{\nu} - (B' + B)J + (B' - B)J^2 \tag{14.5a}$$

$$\text{Q branch } (\Delta J = 0): \quad \tilde{\nu}_Q(J) = \tilde{\nu} + (B' - B)J(J+1) \tag{14.5b}$$

$$\text{R branch } (\Delta J = +1): \quad \tilde{\nu}_R(J) = \tilde{\nu} + (B' + B)(J+1) + (B' - B)(J+1)^2 \tag{14.5c}$$

(These are the analogues of eqn 13.63.) First, suppose that the bond length in the electronically excited state is greater than that in the ground state; then $B' < B$ and $B' - B$ is negative. In this case the lines of the R branch converge with increasing J and when J is such that $|B' - B|(J+1) > B' + B$ the lines start to appear at successively decreasing wavenumbers. That is, the R branch has a **band head** (Fig. 14.11a). When the bond is shorter in the excited state than in the ground state, $B' > B$ and $B' - B$ is positive. In this case, the lines of the P branch begin to converge and go through a head when J is such that $(B' - B)J > B' + B$ (Fig. 14.11b).

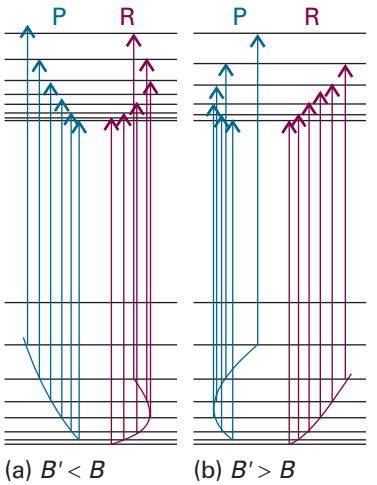

Fig. 14.11 When the rotational constants of a diatomic molecule differ significantly in the initial and final states of an electronic transition, the P and R branches show a head. (a) The formation of a head in the R branch when $B' < B$; (b) the formation of a head in the P branch when $B' > B$.

14.2 The electronic spectra of polyatomic molecules

The absorption of a photon can often be traced to the excitation of specific types of electrons or to electrons that belong to a small group of atoms in a polyatomic molecule. For example, when a carbonyl group (>C=O) is present, an absorption at about 290 nm is normally observed, although its precise location depends on the nature of the rest of the molecule. Groups with characteristic optical absorptions are called **chromophores** (from the Greek for 'colour bringer'), and their presence often accounts for the colours of substances (Table 14.3).

Comment 14.2
The web site for this text contains links to databases of electronic spectra.

(a) *d–d* transitions

In a free atom, all five *d* orbitals of a given shell are degenerate. In a *d*-metal complex, where the immediate environment of the atom is no longer spherical, the *d* orbitals

Synoptic table 14.3* Absorption characteristics ofsome groups and molecules

Group	$\tilde{\nu}$/cm^{-1}	λ_{max}/nm	ε/(dm^3 mol^{-1} cm^{-1})
C=C ($\pi^* \leftarrow \pi$)	61 000	163	5 000
	57 300	174	15 500
C=O ($\pi^* \leftarrow n$)	35 000–37 000	270–290	10–20
H_2O ($\pi^* \leftarrow n$)	60 000	167	7 000

* More values are given in the *Data section*.

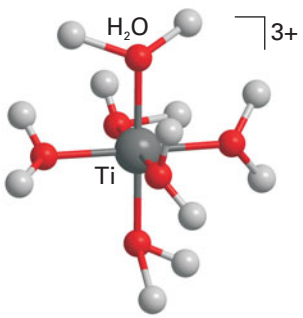

1 $[Ti(OH_2)_6]^{3+}$

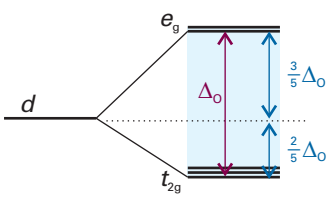

2

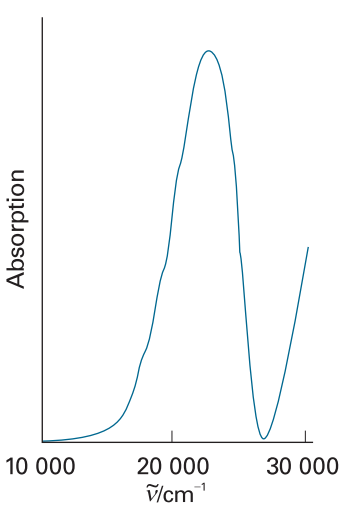

Fig. 14.13 The electronic absorption spectrum of $[Ti(OH_2)_6]^{3+}$ in aqueous solution.

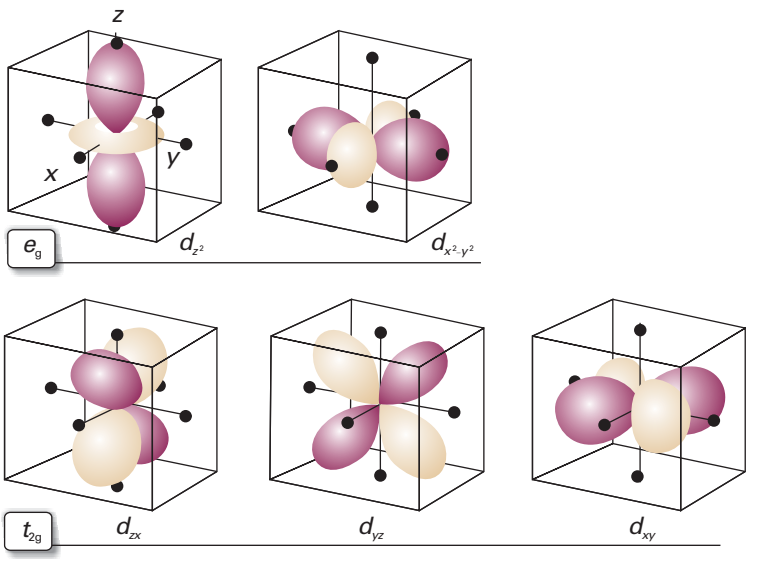

Fig. 14.12 The classification of *d*-orbitals in an octahedral environment.

are not all degenerate, and electrons can absorb energy by making transitions between them. We show in the following *Justification* that in an octahedral complex, such as $[Ti(OH_2)_6]^{3+}$ (**1**), the five *d* orbitals of the central atom are split into two sets (**2**), a triply degenerate set labelled t_{2g} and a doubly degenerate set labelled e_g. The three t_{2g} orbitals lie below the two e_g orbitals; the difference in energy is denoted Δ_O and called the **ligand-field splitting parameter** (the O denoting octahedral symmetry).

Justification 14.3 *The splitting of* d*-orbitals in an octahedral* d*-metal complex*

In an octahedral *d*-metal complex, six identical ions or molecules, the *ligands*, are at the vertices of a regular octahedron, with the metal ion at its centre. The ligands can be regarded as point negative charges that are repelled by the *d*-electrons of the central ion. Figure 14.12 shows the consequence of this arrangement: the five *d*-orbitals fall into two groups, with $d_{x^2-y^2}$ and d_{z^2} pointing directly towards the ligand positions, and d_{xy}, d_{yz}, and d_{zx} pointing between them. An electron occupying an orbital of the former group has a less favourable potential energy than when it occupies any of the three orbitals of the other group, and so the *d*-orbitals split into the two sets shown in (**2**) with an energy difference Δ_O: a triply degenerate set comprising the d_{xy}, d_{yz}, and d_{zx} orbitals and labelled t_{2g}, and a doubly degenerate set comprising the $d_{x^2-y^2}$ and d_{z^2} orbitals and labelled e_g.

The *d*-orbitals also divide into two sets in a tetrahedral complex, but in this case the *e* orbitals lie below the t_2 orbitals and their separation is written Δ_T. Neither Δ_O nor Δ_T is large, so transitions between the two sets of orbitals typically occur in the visible region of the spectrum. The transitions are responsible for many of the colours that are so characteristic of *d*-metal complexes. As an example, the spectrum of $[Ti(OH_2)_6]^{3+}$ near 20 000 cm^{-1} (500 nm) is shown in Fig. 14.13, and can be ascribed to the promotion of its single *d* electron from a t_{2g} orbital to an e_g orbital. The wavenumber of the absorption maximum suggests that $\Delta_O \approx 20\,000\ cm^{-1}$ for this complex, which corresponds to about 2.5 eV.

According to the Laporte rule (Section 14.1b), *d–d* transitions are parity-forbidden in octahedral complexes because they are g → g transitions (more specifically $e_g \leftarrow t_{2g}$ transitions). However, *d–d* transitions become weakly allowed as vibronic transitions as a result of coupling to asymmetrical vibrations such as that shown in Fig. 14.5.

(b) Charge-transfer transitions

A complex may absorb radiation as a result of the transfer of an electron from the ligands into the *d*-orbitals of the central atom, or vice versa. In such **charge-transfer transitions** the electron moves through a considerable distance, which means that the transition dipole moment may be large and the absorption is correspondingly intense. This mode of chromophore activity is shown by the permanganate ion, MnO_4^-, and accounts for its intense violet colour (which arises from strong absorption within the range 420–700 nm). In this oxoanion, the electron migrates from an orbital that is largely confined to the O atom ligands to an orbital that is largely confined to the Mn atom. It is therefore an example of a **ligand-to-metal charge-transfer transition** (LMCT). The reverse migration, a **metal-to-ligand charge-transfer transition** (MLCT), can also occur. An example is the transfer of a *d* electron into the antibonding π orbitals of an aromatic ligand. The resulting excited state may have a very long lifetime if the electron is extensively delocalized over several aromatic rings, and such species can participate in photochemically induced redox reactions (see Section 23.7).

The intensities of charge-transfer transitions are proportional to the square of the transition dipole moment, in the usual way. We can think of the transition moment as a measure of the distance moved by the electron as it migrates from metal to ligand or vice versa, with a large distance of migration corresponding to a large transition dipole moment and therefore a high intensity of absorption. However, because the integrand in the transition dipole is proportional to the product of the initial and final wavefunctions, it is zero unless the two wavefunctions have nonzero values in the same region of space. Therefore, although large distances of migration favour high intensities, the diminished overlap of the initial and final wavefunctions for large separations of metal and ligands favours low intensities (see Problem 14.17). We encounter similar considerations when we examine electron transfer reactions (Chapter 24), which can be regarded as a special type of charge-transfer transition.

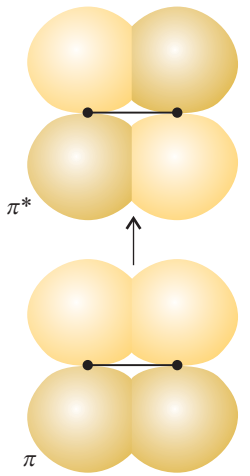

Fig. 14.14 A C=C double bond acts as a chromophore. One of its important transitions is the $\pi^* \leftarrow \pi$ transition illustrated here, in which an electron is promoted from a π orbital to the corresponding antibonding orbital.

(c) $\pi^* \leftarrow \pi$ and $\pi^* \leftarrow n$ transitions

Absorption by a C=C double bond results in the excitation of a π electron into an antibonding π^* orbital (Fig. 14.14). The chromophore activity is therefore due to a $\pi^* \leftarrow \pi$ transition (which is normally read 'π to π-star transition'). Its energy is about 7 eV for an unconjugated double bond, which corresponds to an absorption at 180 nm (in the ultraviolet). When the double bond is part of a conjugated chain, the energies of the molecular orbitals lie closer together and the $\pi^* \leftarrow \pi$ transition moves to longer wavelength; it may even lie in the visible region if the conjugated system is long enough. An important example of an $\pi^* \leftarrow \pi$ transition is provided by the photochemical mechanism of vision (*Impact I14.1*).

The transition responsible for absorption in carbonyl compounds can be traced to the lone pairs of electrons on the O atom. The Lewis concept of a 'lone pair' of electrons is represented in molecular orbital theory by a pair of electrons in an orbital confined largely to one atom and not appreciably involved in bond formation. One of these electrons may be excited into an empty π^* orbital of the carbonyl group (Fig. 14.15), which gives rise to a $\pi^* \leftarrow n$ transition (an 'n to π-star transition'). Typical absorption energies are about 4 eV (290 nm). Because $\pi^* \leftarrow n$ transitions in carbonyls are symmetry forbidden, the absorptions are weak.

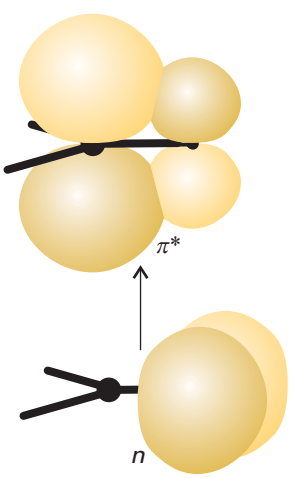

Fig. 14.15 A carbonyl group (C=O) acts as a chromophore primarily on account of the excitation of a nonbonding O lone-pair electron to an antibonding CO π orbital.

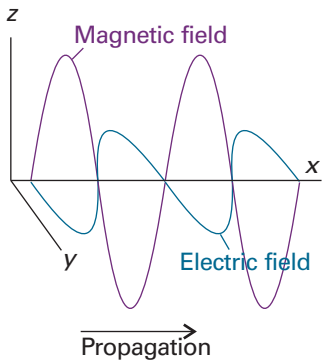

Fig. 14.16 Electromagnetic radiation consists of a wave of electric and magnetic fields perpendicular to the direction of propagation (in this case the *x*-direction), and mutually perpendicular to each other. This illustration shows a plane-polarized wave, with the electric and magnetic fields oscillating in the *xy* and *xz* planes, respectively.

(d) Circular dichroism spectroscopy

Electronic spectra can reveal additional details of molecular structure when experiments are conducted with **polarized light**, electromagnetic radiation with electric and magnetic fields that oscillate only in certain directions. Light is **plane polarized** when the electric and magnetic fields each oscillate in a single plane (Fig. 14.16). The plane of polarization may be oriented in any direction around the direction of propagation (the *x*-direction in Fig. 14.16), with the electric and magnetic fields perpendicular to that direction (and perpendicular to each other). An alternative mode of polarization is **circular polarization**, in which the electric and magnetic fields rotate around the direction of propagation in either a clockwise or a counter-clockwise sense but remain perpendicular to it and each other.

When plane-polarized radiation passes through samples of certain kinds of matter, the plane of polarization is rotated around the direction of propagation. This rotation is the familiar phenomenon of optical activity, observed when the molecules in the sample are chiral (Section 12.3b). Chiral molecules have a second characteristic: they absorb left and right circularly polarized light to different extents. In a circularly polarized ray of light, the electric field describes a helical path as the wave travels through space (Fig. 14.17), and the rotation may be either clockwise or counterclockwise. The differential absorption of left- and right-circularly polarized light is called **circular dichroism**. In terms of the absorbances for the two components, A_L and A_R, the circular dichroism of a sample of molar concentration [J] is reported as

$$\Delta\varepsilon = \varepsilon_L - \varepsilon_R = \frac{A_L - A_R}{[J]l} \tag{14.6}$$

where l is the path length of the sample.

Circular dichroism is a useful adjunct to visible and UV spectroscopy. For example, the CD spectra of the enantiomeric pairs of chiral *d*-metal complexes are distinctly different, whereas there is little difference between their absorption spectra (Fig. 14.18). Moreover, CD spectra can be used to assign the absolute configuration of complexes by comparing the observed spectrum with the CD spectrum of a similar complex of known handedness. We shall see in Chapter 19 that the CD spectra of biological polymers, such as proteins and nucleic acids, give similar structural information. In these cases the spectrum of the polymer chain arises from the chirality of individual monomer units and, in addition, a contribution from the three-dimensional structure of the polymer itself.

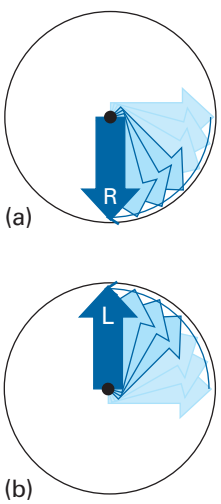

Fig. 14.17 In circularly polarized light, the electric field at different points along the direction of propagation rotates. The arrays of arrows in these illustrations show the view of the electric field when looking toward the oncoming ray: (a) right-circularly polarized, (b) left-circularly polarized light.

IMPACT ON BIOCHEMISTRY

I14.1 Vision

The eye is an exquisite photochemical organ that acts as a transducer, converting radiant energy into electrical signals that travel along neurons. Here we concentrate on the events taking place in the human eye, but similar processes occur in all animals. Indeed, a single type of protein, rhodopsin, is the primary receptor for light throughout the animal kingdom, which indicates that vision emerged very early in evolutionary history, no doubt because of its enormous value for survival.

Photons enter the eye through the cornea, pass through the ocular fluid that fills the eye, and fall on the retina. The ocular fluid is principally water, and passage of light through this medium is largely responsible for the *chromatic aberration* of the eye, the blurring of the image as a result of different frequencies being brought to slightly different focuses. The chromatic aberration is reduced to some extent by the tinted region called the *macular pigment* that covers part of the retina. The pigments in this region are the carotene-like xanthophylls (**3**), which absorb some of the blue light and

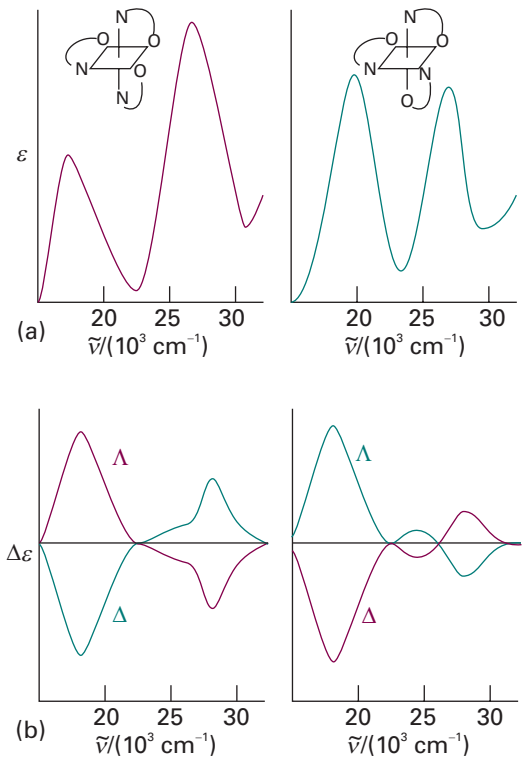

Fig. 14.18 (a) The absorption spectra of two isomers, denoted mer and fac, of $[Co(ala)_3]$, where ala is the conjugate base of alanine, and (b) the corresponding CD spectra. The left- and right-handed forms of these isomers give identical absorption spectra. However, the CD spectra are distinctly different, and the absolute configurations (denoted Λ and Δ) have been assigned by comparison with the CD spectra of a complex of known absolute configuration.

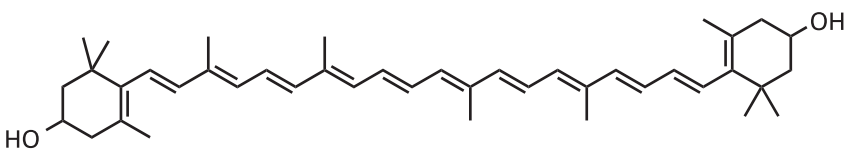

3 A xanthophyll

hence help to sharpen the image. They also protect the photoreceptor molecules from too great a flux of potentially dangerous high energy photons. The xanthophylls have delocalized electrons that spread along the chain of conjugated double bonds, and the $\pi^* \leftarrow \pi$ transition lies in the visible.

About 57 per cent of the photons that enter the eye reach the retina; the rest are scattered or absorbed by the ocular fluid. Here the primary act of vision takes place, in which the chromophore of a rhodopsin molecule absorbs a photon in another $\pi^* \leftarrow \pi$ transition. A rhodopsin molecule consists of an opsin protein molecule to which is attached a 11-*cis*-retinal molecule (**4**). The latter resembles half a carotene molecule, showing Nature's economy in its use of available materials. The attachment is by the formation of a protonated Schiff's base, utilizing the —CHO group of the chromophore and the terminal NH_2 group of the sidechain, a lysine residue from opsin. The free 11-*cis*-retinal molecule absorbs in the ultraviolet, but attachment to the opsin protein molecule shifts the absorption into the visible region. The rhodopsin molecules are situated in the membranes of special cells (the 'rods' and the 'cones') that cover the retina. The opsin molecule is anchored into the cell membrane by two hydrophobic groups and largely surrounds the chromophore (Fig. 14.19).

Immediately after the absorption of a photon, the 11-*cis*-retinal molecule undergoes photoisomerization into all-*trans*-retinal (**5**). Photoisomerization takes about

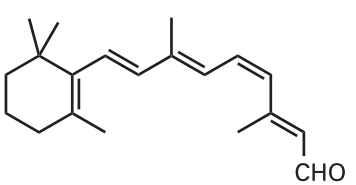

4 11-*cis*-retinal

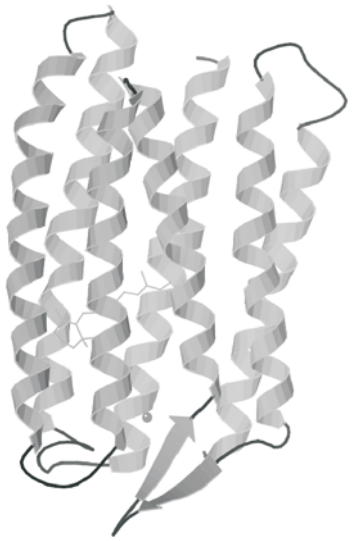

Fig. 14.19 The structure of the rhodopsin molecule, consisting of an opsin protein to which is attached an 11-*cis*-retinal molecule embedded in the space surrounded by the helical regions.

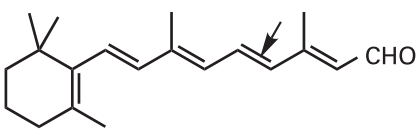

5 All-*trans*-retinal

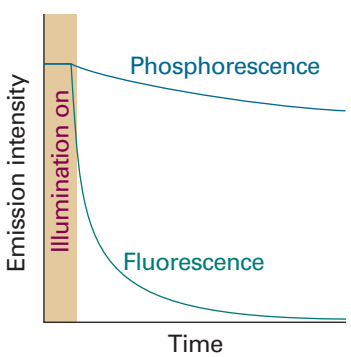

Fig. 14.20 The empirical (observation-based) distinction between fluorescence and phosphorescence is that the former is extinguished very quickly after the exciting source is removed, whereas the latter continues with relatively slowly diminishing intensity.

200 fs and about 67 pigment molecules isomerize for every 100 photons that are absorbed. The process occurs because the $\pi^* \leftarrow \pi$ excitation of an electron loosens one of the π-bonds (the one indicated by the arrow in **5**), its torsional rigidity is lost, and one part of the molecule swings round into its new position. At that point, the molecule returns to its ground state, but is now trapped in its new conformation. The straightened tail of all-*trans*-retinal results in the molecule taking up more space than 11-*cis*-retinal did, so the molecule presses against the coils of the opsin molecule that surrounds it. In about 0.25–0.50 ms from the initial absorption event, the rhodopsin molecule is activated both by the isomerization of retinal and deprotonation of its Schiff's base tether to opsin, forming an intermediate known as *metarhodopsin II*.

In a sequence of biochemical events known as the *biochemical cascade*, metarhodopsin II activates the protein transducin, which in turn activates a phosphodiesterase enzyme that hydrolyses cyclic guanine monophosphate (cGMP) to GMP. The reduction in the concentration of cGMP causes ion channels, proteins that mediate the movement of ions across biological membranes, to close and the result is a sizable change in the transmembrane potential (see *Impact I7.2* for a discussion of transmembrane potentials). The pulse of electric potential travels through the optical nerve and into the optical cortex, where it is interpreted as a signal and incorporated into the web of events we call 'vision'.

The resting state of the rhodopsin molecule is restored by a series of nonradiative chemical events powered by ATP. The process involves the escape of all-*trans*-retinal as all-*trans*-retinol (in which —CHO has been reduced to $-CH_2OH$) from the opsin molecule by a process catalysed by the enzyme rhodopsin kinase and the attachment of another protein molecule, arrestin. The free all-*trans*-retinol molecule now undergoes enzyme-catalysed isomerization into 11-*cis*-retinol followed by dehydrogenation to form 11-*cis*-retinal, which is then delivered back into an opsin molecule. At this point, the cycle of excitation, photoisomerization, and regeneration is ready to begin again.

The fates of electronically excited states

A **radiative decay process** is a process in which a molecule discards its excitation energy as a photon. A more common fate is **nonradiative decay**, in which the excess energy is transferred into the vibration, rotation, and translation of the surrounding molecules. This thermal degradation converts the excitation energy completely into thermal motion of the environment (that is, to 'heat'). An excited molecule may also take part in a chemical reaction, as we discuss in Chapter 23.

14.3 Fluorescence and phosphorescence

In **fluorescence**, spontaneous emission of radiation occurs within a few nanoseconds after the exciting radiation is extinguished (Fig. 14.20). In **phosphorescence**, the spontaneous emission may persist for long periods (even hours, but characteristically seconds or fractions of seconds). The difference suggests that fluorescence is a fast conversion of absorbed radiation into re-emitted energy, and that phosphorescence involves the storage of energy in a reservoir from which it slowly leaks.

(a) Fluorescence

Figure 14.21 shows the sequence of steps involved in fluorescence. The initial absorption takes the molecule to an excited electronic state, and if the absorption spectrum were monitored it would look like the one shown in Fig. 14.22a. The excited molecule

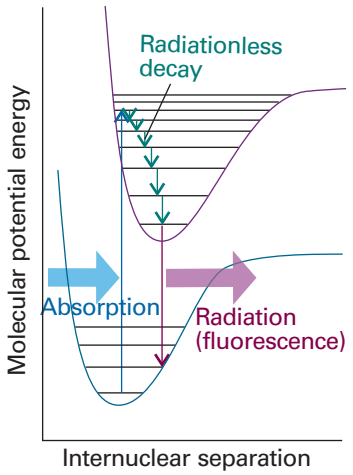

Fig. 14.21 The sequence of steps leading to fluorescence. After the initial absorption, the upper vibrational states undergo radiationless decay by giving up energy to the surroundings. A radiative transition then occurs from the vibrational ground state of the upper electronic state.

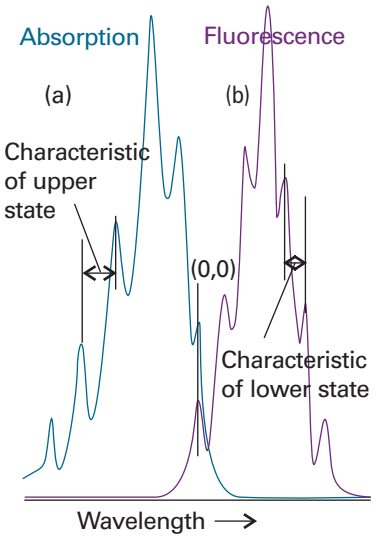

Fig. 14.22 An absorption spectrum (a) shows a vibrational structure characteristic of the upper state. A fluorescence spectrum (b) shows a structure characteristic of the lower state; it is also displaced to lower frequencies (but the 0–0 transitions are coincident) and resembles a mirror image of the absorption.

is subjected to collisions with the surrounding molecules, and as it gives up energy nonradiatively it steps down the ladder of vibrational levels to the lowest vibrational level of the electronically excited molecular state. The surrounding molecules, however, might now be unable to accept the larger energy difference needed to lower the molecule to the ground electronic state. It might therefore survive long enough to undergo spontaneous emission, and emit the remaining excess energy as radiation. The downward electronic transition is vertical (in accord with the Franck–Condon principle) and the fluorescence spectrum has a vibrational structure characteristic of the *lower* electronic state (Fig. 14.22b).

Provided they can be seen, the 0–0 absorption and fluorescence transitions can be expected to be coincident. The absorption spectrum arises from 1–0, 2–0, . . . transitions that occur at progressively higher wavenumber and with intensities governed by the Franck–Condon principle. The fluorescence spectrum arises from 0–0, 0–1, . . . *downward* transitions that hence occur with decreasing wavenumbers. The 0–0 absorption and fluorescence peaks are not always exactly coincident, however, because the solvent may interact differently with the solute in the ground and excited states (for instance, the hydrogen bonding pattern might differ). Because the solvent molecules do not have time to rearrange during the transition, the absorption occurs in an environment characteristic of the solvated ground state; however, the fluorescence occurs in an environment characteristic of the solvated excited state (Fig. 14.23).

Fluorescence occurs at lower frequencies (longer wavelengths) than the incident radiation because the emissive transition occurs after some vibrational energy has been discarded into the surroundings. The vivid oranges and greens of fluorescent dyes are an everyday manifestation of this effect: they absorb in the ultraviolet and blue, and fluoresce in the visible. The mechanism also suggests that the intensity of the fluorescence ought to depend on the ability of the solvent molecules to accept the

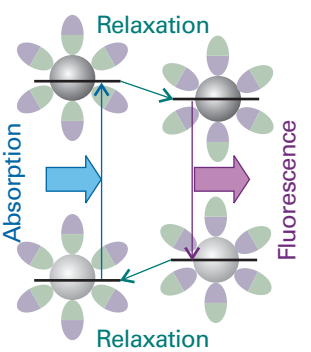

Fig. 14.23 The solvent can shift the fluorescence spectrum relative to the absorption spectrum. On the left we see that the absorption occurs with the solvent (the ellipses) in the arrangement characteristic of the ground electronic state of the molecule (the sphere). However, before fluorescence occurs, the solvent molecules relax into a new arrangement, and that arrangement is preserved during the subsequent radiative transition.

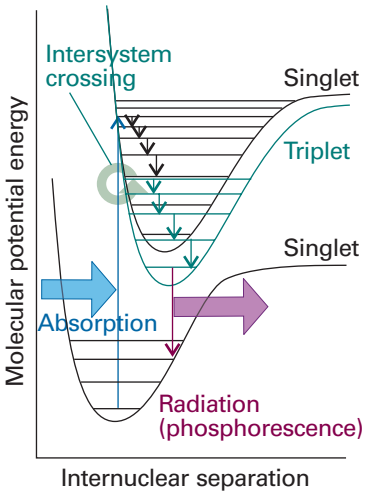

Fig. 14.24 The sequence of steps leading to phosphorescence. The important step is the intersystem crossing, the switch from a singlet state to a triplet state brought about by spin–orbit coupling. The triplet state acts as a slowly radiating reservoir because the return to the ground state is spin-forbidden.

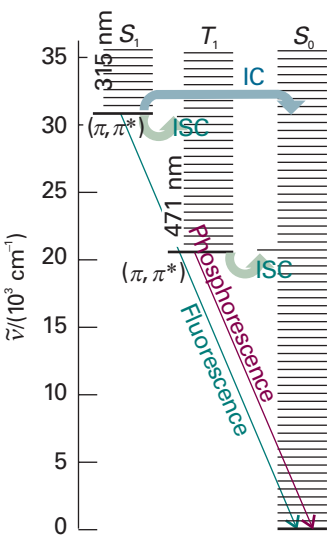

Fig. 14.25 A Jablonski diagram (here, for naphthalene) is a simplified portrayal of the relative positions of the electronic energy levels of a molecule. Vibrational levels of states of a given electronic state lie above each other, but the relative horizontal locations of the columns bear no relation to the nuclear separations in the states. The ground vibrational states of each electronic state are correctly located vertically but the other vibrational states are shown only schematically. (IC: internal conversion; ISC: intersystem crossing.)

electronic and vibrational quanta. It is indeed found that a solvent composed of molecules with widely spaced vibrational levels (such as water) can in some cases accept the large quantum of electronic energy and so extinguish, or 'quench', the fluorescence. We examine the mechanisms of fluorescence quenching in Chapter 23.

(b) Phosphorescence

Figure 14.24 shows the sequence of events leading to phosphorescence for a molecule with a singlet ground state. The first steps are the same as in fluorescence, but the presence of a triplet excited state plays a decisive role. The singlet and triplet excited states share a common geometry at the point where their potential energy curves intersect. Hence, if there is a mechanism for unpairing two electron spins (and achieving the conversion of $\uparrow\downarrow$ to $\uparrow\uparrow$), the molecule may undergo **intersystem crossing**, a nonradiative transition between states of different multiplicity, and become a triplet state. We saw in the discussion of atomic spectra (Section 10.9d) that singlet–triplet transitions may occur in the presence of spin–orbit coupling, and the same is true in molecules. We can expect intersystem crossing to be important when a molecule contains a moderately heavy atom (such as S), because then the spin–orbit coupling is large.

If an excited molecule crosses into a triplet state, it continues to deposit energy into the surroundings. However, it is now stepping down the triplet's vibrational ladder, and at the lowest energy level it is trapped because the triplet state is at a lower energy than the corresponding singlet (recall Hund's rule, Section 13.7). The solvent cannot absorb the final, large quantum of electronic excitation energy, and the molecule cannot radiate its energy because return to the ground state is spin-forbidden (Section 14.1). The radiative transition, however, is not totally forbidden because the spin–orbit coupling that was responsible for the intersystem crossing also breaks the selection rule. The molecules are therefore able to emit weakly, and the emission may continue long after the original excited state was formed.

The mechanism accounts for the observation that the excitation energy seems to get trapped in a slowly leaking reservoir. It also suggests (as is confirmed experimentally) that phosphorescence should be most intense from solid samples: energy transfer is then less efficient and intersystem crossing has time to occur as the singlet excited state steps slowly past the intersection point. The mechanism also suggests that the phosphorescence efficiency should depend on the presence of a moderately heavy atom (with strong spin–orbit coupling), which is in fact the case. The confirmation of the mechanism is the experimental observation (using the sensitive magnetic resonance techniques described in Chapter 15) that the sample is paramagnetic while the reservoir state, with its unpaired electron spins, is populated.

The various types of nonradiative and radiative transitions that can occur in molecules are often represented on a schematic **Jablonski diagram** of the type shown in Fig. 14.25.

IMPACT ON BIOCHEMISTRY

I14.2 Fluorescence microscopy

Apart from a small number of co-factors, such as the chlorophylls and flavins, the majority of the building blocks of proteins and nucleic acids do not fluoresce strongly. Four notable exceptions are the amino acids tryptophan ($\lambda_{abs} \approx 280$ nm and $\lambda_{fluor} \approx 348$ nm in water), tyrosine ($\lambda_{abs} \approx 274$ nm and $\lambda_{fluor} \approx 303$ nm in water), and phenylalanine ($\lambda_{abs} \approx 257$ nm and $\lambda_{fluor} \approx 282$ nm in water), and the oxidized form of the sequence serine–tyrosine–glycine (**6**) found in the green fluorescent protein (GFP) of certain jellyfish. The wild type of GFP from *Aequora victoria* absorbs strongly at 395 nm and emits maximally at 509 nm.

In **fluorescence microscopy**, images of biological cells at work are obtained by attaching a large number of fluorescent molecules to proteins, nucleic acids, and membranes and then measuring the distribution of fluorescence intensity within the illuminated area. A common fluorescent label is GFP. With proper filtering to remove light due to Rayleigh scattering of the incident beam, it is possible to collect light from the sample that contains only fluorescence from the label. However, great care is required to eliminate fluorescent impurities from the sample.

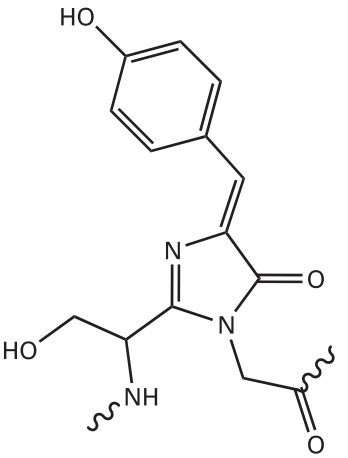

6 The chromophore of GFP

14.4 Dissociation and predissociation

Another fate for an electronically excited molecule is **dissociation**, the breaking of bonds (Fig. 14.26). The onset of dissociation can be detected in an absorption spectrum by seeing that the vibrational structure of a band terminates at a certain energy. Absorption occurs in a continuous band above this **dissociation limit** because the final state is an unquantized translational motion of the fragments. Locating the dissociation limit is a valuable way of determining the bond dissociation energy.

In some cases, the vibrational structure disappears but resumes at higher photon energies. This **predissociation** can be interpreted in terms of the molecular potential energy curves shown in Fig. 14.27. When a molecule is excited to a vibrational level, its electrons may undergo a redistribution that results in it undergoing an **internal conversion**, a radiationless conversion to another state of the same multiplicity. An internal conversion occurs most readily at the point of intersection of the two molecular potential energy curves, because there the nuclear geometries of the two states are the same. The state into which the molecule converts may be dissociative, so the states near the intersection have a finite lifetime, and hence their energies are imprecisely defined. As a result, the absorption spectrum is blurred in the vicinity of the intersection. When the incoming photon brings enough energy to excite the molecule

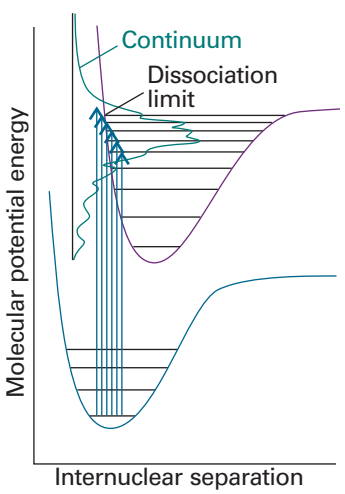

Fig. 14.26 When absorption occurs to unbound states of the upper electronic state, the molecule dissociates and the absorption is a continuum. Below the dissociation limit the electronic spectrum shows a normal vibrational structure.

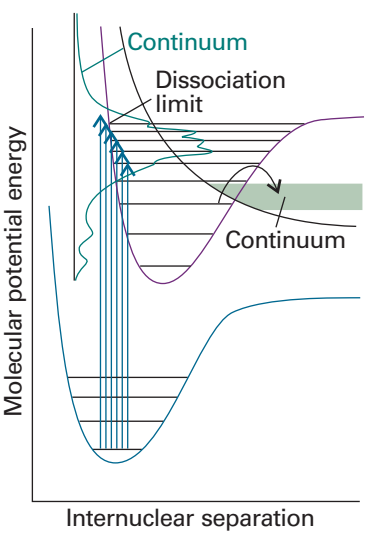

Fig. 14.27 When a dissociative state crosses a bound state, as in the upper part of the illustration, molecules excited to levels near the crossing may dissociate. This process is called predissociation, and is detected in the spectrum as a loss of vibrational structure that resumes at higher frequencies.

to a vibrational level high above the intersection, the internal conversion does not occur (the nuclei are unlikely to have the same geometry). Consequently, the levels resume their well-defined, vibrational character with correspondingly well-defined energies, and the line structure resumes on the high-frequency side of the blurred region.

Lasers

Lasers have transformed chemistry as much as they have transformed the everyday world. They lie very much on the frontier of physics and chemistry, for their operation depends on details of optics and, in some cases, of solid-state processes. In this section, we discuss the mechanisms of laser action, and then explore their applications in chemistry. In *Further information 14.1*, we discuss the modes of operation of a number of commonly available laser systems.

14.5 General principles of laser action

The word laser is an acronym formed from **l**ight **a**mplification by **s**timulated **e**mission of **r**adiation. In stimulated emission, an excited state is stimulated to emit a photon by radiation of the same frequency; the more photons that are present, the greater the probability of the emission. The essential feature of laser action is positive-feedback: the more photons present of the appropriate frequency, the more photons of that frequency that will be stimulated to form.

(a) Population inversion

One requirement of laser action is the existence of a **metastable excited state**, an excited state with a long enough lifetime for it to participate in stimulated emission. Another requirement is the existence of a greater population in the metastable state than in the lower state where the transition terminates, for then there will be a net emission of radiation. Because at thermal equilibrium the opposite is true, it is necessary to achieve a **population inversion** in which there are more molecules in the upper state than in the lower.

One way of achieving population inversion is illustrated in Fig. 14.28. The molecule is excited to an intermediate state I, which then gives up some of its energy nonradiatively and changes into a lower state A; the laser transition is the return of A to the ground state X. Because three energy levels are involved overall, this arrangement leads to a **three-level laser**. In practice, I consists of many states, all of which can convert to the upper of the two laser states A. The $I \leftarrow X$ transition is stimulated with an intense flash of light in the process called **pumping**. The pumping is often achieved with an electric discharge through xenon or with the light of another laser. The conversion of I to A should be rapid, and the laser transitions from A to X should be relatively slow.

The disadvantage of this three-level arrangement is that it is difficult to achieve population inversion, because so many ground-state molecules must be converted to the excited state by the pumping action. The arrangement adopted in a **four-level laser** simplifies this task by having the laser transition terminate in a state A' other than the ground state (Fig. 14.29). Because A' is unpopulated initially, any population in A corresponds to a population inversion, and we can expect laser action if A is sufficiently metastable. Moreover, this population inversion can be maintained if the $A' \leftarrow X$ transitions are rapid, for these transitions will deplete any population in A' that stems from the laser transition, and keep the state A' relatively empty.

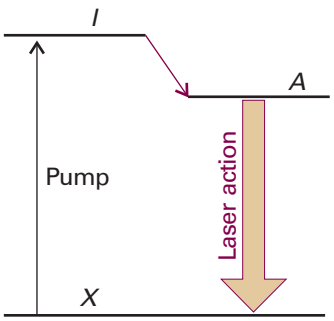

Fig. 14.28 The transitions involved in one kind of three-level laser. The pumping pulse populates the intermediate state I, which in turn populates the laser state A. The laser transition is the stimulated emission $A \rightarrow X$.

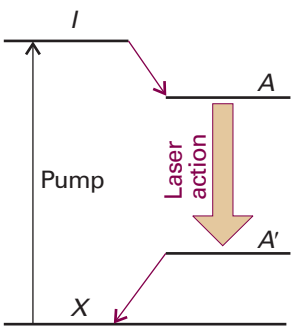

Fig. 14.29 The transitions involved in a four-level laser. Because the laser transition terminates in an excited state (A'), the population inversion between A and A' is much easier to achieve.

(b) Cavity and mode characteristics

The laser medium is confined to a cavity that ensures that only certain photons of a particular frequency, direction of travel, and state of polarization are generated abundantly. The cavity is essentially a region between two mirrors, which reflect the light back and forth. This arrangement can be regarded as a version of the particle in a box, with the particle now being a photon. As in the treatment of a particle in a box (Section 9.1), the only wavelengths that can be sustained satisfy

$$n \times \tfrac{1}{2}\lambda = L \tag{14.7}$$

where n is an integer and L is the length of the cavity. That is, only an integral number of half-wavelengths fit into the cavity; all other waves undergo destructive interference with themselves. In addition, not all wavelengths that can be sustained by the cavity are amplified by the laser medium (many fall outside the range of frequencies of the laser transitions), so only a few contribute to the laser radiation. These wavelengths are the **resonant modes** of the laser.

Photons with the correct wavelength for the resonant modes of the cavity and the correct frequency to stimulate the laser transition are highly amplified. One photon might be generated spontaneously, and travel through the medium. It stimulates the emission of another photon, which in turn stimulates more (Fig. 14.30). The cascade of energy builds up rapidly, and soon the cavity is an intense reservoir of radiation at all the resonant modes it can sustain. Some of this radiation can be withdrawn if one of the mirrors is partially transmitting.

The resonant modes of the cavity have various natural characteristics, and to some extent may be selected. Only photons that are travelling strictly parallel to the axis of the cavity undergo more than a couple of reflections, so only they are amplified, all others simply vanishing into the surroundings. Hence, laser light generally forms a beam with very low divergence. It may also be polarized, with its electric vector in a particular plane (or in some other state of polarization), by including a polarizing filter into the cavity or by making use of polarized transitions in a solid medium.

Laser radiation is **coherent** in the sense that the electromagnetic waves are all in step. In **spatial coherence** the waves are in step across the cross-section of the beam emerging from the cavity. In **temporal coherence** the waves remain in step along the beam. The latter is normally expressed in terms of a **coherence length**, l_C, the distance over which the waves remain coherent, and is related to the range of wavelengths, $\Delta\lambda$ present in the beam:

$$l_C = \frac{\lambda^2}{2\Delta\lambda} \tag{14.8}$$

If the beam were perfectly monochromatic, with strictly one wavelength present, $\Delta\lambda$ would be zero and the waves would remain in step for an infinite distance. When many wavelengths are present, the waves get out of step in a short distance and the coherence length is small. A typical light bulb gives out light with a coherence length of only about 400 nm; a He–Ne laser with $\Delta\lambda \approx 2$ pm has a coherence length of about 10 cm.

(c) *Q*-switching

A laser can generate radiation for as long as the population inversion is maintained. A laser can operate continuously when heat is easily dissipated, for then the population of the upper level can be replenished by pumping. When overheating is a problem, the laser can be operated only in pulses, perhaps of microsecond or millisecond duration, so that the medium has a chance to cool or the lower state discard its population.

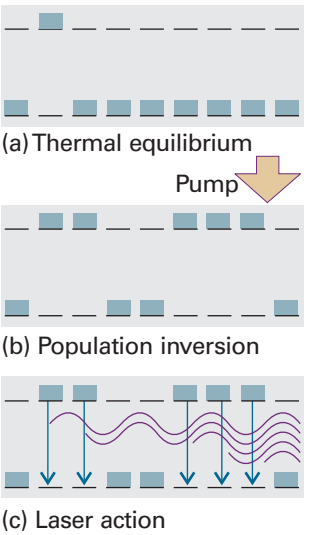

Fig. 14.30 A schematic illustration of the steps leading to laser action. (a) The Boltzmann population of states (see *Molecular interpretation* 3.1), with more atoms in the ground state. (b) When the initial state absorbs, the populations are inverted (the atoms are pumped to the excited state). (c) A cascade of radiation then occurs, as one emitted photon stimulates another atom to emit, and so on. The radiation is coherent (phases in step).

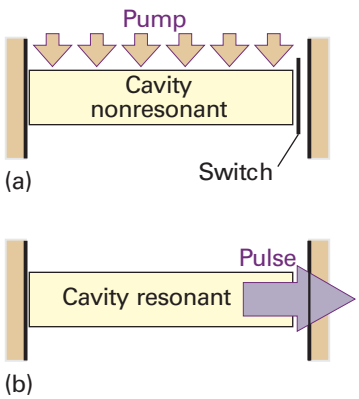

Fig. 14.31 The principle of *Q*-switching. The excited state is populated while the cavity is nonresonant. Then the resonance characteristics are suddenly restored, and the stimulated emission emerges in a giant pulse.

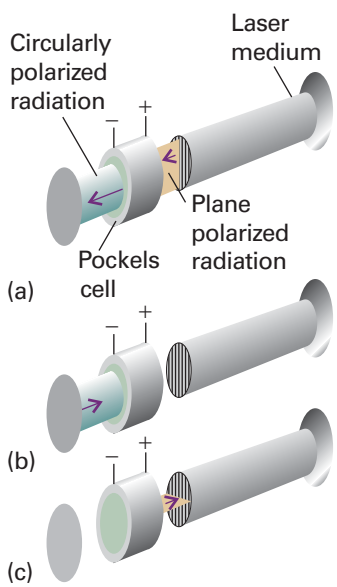

Fig. 14.32 The principle of a Pockels cell. When light passes through a cell that is 'on', its plane of polarization is rotated and so the laser cavity is non-resonant (its *Q*-factor is reduced). In this sequence, (a) the plane polarized ray becomes circularly polarized, (b) is reflected, and (c) emerges from the Pockels cell with perpendicular plane polarization. When the cell is turned off, no change of polarization occurs, and the cavity becomes resonant.

However, it is sometimes desirable to have pulses of radiation rather than a continuous output, with a lot of power concentrated into a brief pulse. One way of achieving pulses is by **Q-switching**, the modification of the resonance characteristics of the laser cavity. The name comes from the '*Q*-factor' used as a measure of the quality of a resonance cavity in microwave engineering.

Example 14.2 *Relating the power and energy of a laser*

A laser rated at 0.10 J can generate radiation in 3.0 ns pulses at a pulse repetition rate of 10 Hz. Assuming that the pulses are rectangular, calculate the peak power output and the average power output of this laser.

Method The power output is the energy released in an interval divided by the duration of the interval, and is expressed in watts (1 W = 1 J s^{-1}). To calculate the peak power output, P_{peak}, we divide the energy released during the pulse divided by the duration of the pulse. The average power output, $P_{average}$, is the total energy released by a large number of pulses divided by the duration of the time interval over which the total energy was measured. So, the average power is simply the energy released by one pulse multiplied by the pulse repetition rate.

Answer From the data,

$$P_{peak} = \frac{0.10\ \text{J}}{3.0 \times 10^{-9}\ \text{s}} = 3.3 \times 10^{7}\ \text{J s}^{-1}$$

That is, the peak power output is 33 MW. The pulse repetition rate is 10 Hz, so ten pulses are emitted by the laser for every second of operation. It follows that the average power output is

$$P_{average} = 0.10\ \text{J} \times 10\ \text{s}^{-1} = 1.0\ \text{J s}^{-1} = 1.0\ \text{W}$$

The peak power is much higher than the average power because this laser emits light for only 30 ns during each second of operation.

Self-test 14.3 Calculate the peak power and average power output of a laser with a pulse energy of 2.0 mJ, a pulse duration of 30 ps, and a pulse repetition rate of 38 MHz. [P_{peak} = 67 MW, $P_{average}$ = 76 kW]

The aim of *Q*-switching is to achieve a healthy population inversion in the absence of the resonant cavity, then to plunge the population-inverted medium into a cavity, and hence to obtain a sudden pulse of radiation. The switching may be achieved by impairing the resonance characteristics of the cavity in some way while the pumping pulse is active, and then suddenly to improve them (Fig. 14.31). One technique is to use a **Pockels cell**, which is an electro-optical device based on the ability of some crystals, such as those of potassium dihydrogenphosphate (KH_2PO_4), to convert plane-polarized light to circularly polarized light when an electrical potential difference is applied. If a Pockels cell is made part of a laser cavity, then its action and the change in polarization that occurs when light is reflected from a mirror convert light polarized in one plane into reflected light polarized in the perpendicular plane (Fig. 14.32). As a result, the reflected light does not stimulate more emission. However, if the cell is suddenly turned off, the polarization effect is extinguished and all the energy stored in the cavity can emerge as an intense pulse of stimulated emission. An alternative technique is to use a **saturable absorber**, typically a solution of a dye that loses its ability

to absorb when many of its molecules have been excited by intense radiation. The dye then suddenly becomes transparent and the cavity becomes resonant. In practice, Q-switching can give pulses of about 5 ns duration.

(d) Mode locking

The technique of **mode locking** can produce pulses of picosecond duration and less. A laser radiates at a number of different frequencies, depending on the precise details of the resonance characteristics of the cavity and in particular on the number of half-wavelengths of radiation that can be trapped between the mirrors (the cavity modes). The resonant modes differ in frequency by multiples of $c/2L$ (as can be inferred from eqn 14.8 with $\nu = c/\lambda$). Normally, these modes have random phases relative to each other. However, it is possible to lock their phases together. Then interference occurs to give a series of sharp peaks, and the energy of the laser is obtained in short bursts (Fig. 14.33). The sharpness of the peaks depends on the range of modes superimposed, and the wider the range, the narrower the pulses. In a laser with a cavity of length 30 cm, the peaks are separated by 2 ns. If 1000 modes contribute, the width of the pulses is 4 ps.

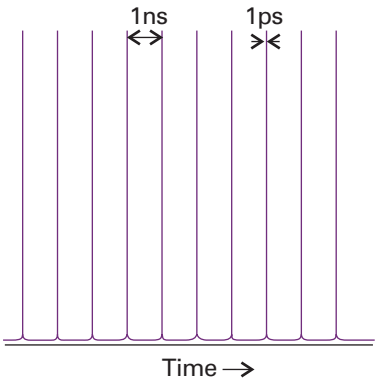

Fig. 14.33 The output of a mode-locked laser consists of a stream of very narrow pulses separated by an interval equal to the time it takes for light to make a round trip inside the cavity.

Justification 14.4 *The origin of mode locking*

The general expression for a (complex) wave of amplitude $\mathcal{E}_0$ and frequency ω is $\mathcal{E}_0 e^{i\omega t}$. Therefore, each wave that can be supported by a cavity of length L has the form

$$\mathcal{E}_n(t) = \mathcal{E}_0 e^{2\pi(\nu + nc/2L)t}$$

where ν is the lowest frequency. A wave formed by superimposing N modes with $n = 0, 1, \ldots, N-1$ has the form

$$\mathcal{E}(t) = \sum_{n=0}^{N-1} \mathcal{E}_n(t) = \mathcal{E}_0 e^{2\pi i \nu t} \sum_{n=0}^{N-1} e^{i\pi nct/L}$$

The sum is a geometrical progression:

$$\sum_{n=0}^{N-1} e^{i\pi nct/L} = 1 + e^{i\pi ct/L} + e^{2i\pi ct/L} + \cdots$$
$$= \frac{\sin(N\pi ct/2L)}{\sin(\pi ct/2L)} \times e^{(N-1)i\pi ct/2L}$$

The intensity, I, of the radiation is proportional to the square modulus of the total amplitude, so

$$I \propto \mathcal{E}^* \mathcal{E} = \mathcal{E}_0^2 \frac{\sin^2(N\pi ct/2L)}{\sin^2(\pi ct/2L)}$$

This function is shown in Fig. 14.34. We see that it is a series of peaks with maxima separated by $t = 2L/c$, the round-trip transit time of the light in the cavity, and that the peaks become sharper as N is increased.

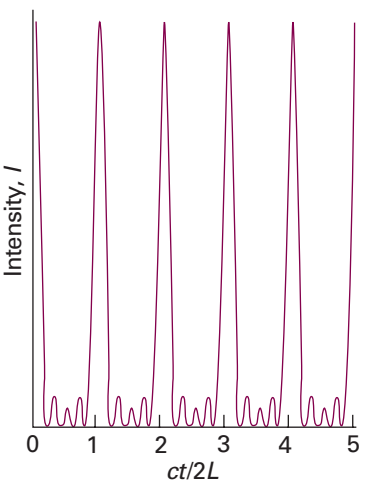

Fig. 14.34 The function derived in *Justification 14.4* showing in more detail the structure of the pulses generated by a mode-locked laser.

Mode locking is achieved by varying the Q-factor of the cavity periodically at the frequency $c/2L$. The modulation can be pictured as the opening of a shutter in synchrony with the round-trip travel time of the photons in the cavity, so only photons making the journey in that time are amplified. The modulation can be achieved by linking a prism in the cavity to a transducer driven by a radiofrequency source at a frequency $c/2L$. The transducer sets up standing-wave vibrations in the prism and modulates the

Table 14.4 Characteristics of laser radiation and their chemical applications

Characteristic	Advantage	Application
High power	Multiphoton process	Nonlinear spectroscopy Saturation spectroscopy
	Low detector noise High scattering intensity	Improved sensitivity Raman spectroscopy
Monochromatic	High resolution State selection	Spectroscopy Isotope separation Photochemically precise State-to-state reaction dynamics
Collimated beam	Long path lengths Forward-scattering observable	Sensitivitv Nonlinear Raman spectroscopy
Coherent	Interference between separate beams	CARS
Pulsed	Precise timing of excitation	Fast reactions Relaxation Energy transfer

loss it introduces into the cavity. We also see in Section 20.10c that the unique optical properties of some materials can be exploited to bring about mode-locking.

14.6 Applications of lasers in chemistry

Laser radiation has five striking characteristics (Table 14.4). Each of them (sometimes in combination with the others) opens up interesting opportunities in spectroscopy, giving rise to 'laser spectroscopy' and, in photochemistry, giving rise to 'laser photochemistry'. What follows is only an initial listing of applications of lasers to chemistry. We see throughout the text how lasers are also used in the study of macromolecules (Chapter 19) and reaction dynamics (Chapter 24).

(a) Multiphoton spectroscopy

The large number of photons in an incident beam generated by a laser gives rise to a qualitatively different branch of spectroscopy, for the photon density is so high that more than one photon may be absorbed by a single molecule and give rise to **multiphoton processes**. One application of multiphoton processes is that states inaccessible by conventional one-photon spectroscopy become observable because the overall transition occurs with no change of parity. For example, in one-photon spectroscopy, only $g \leftrightarrow u$ transitions are observable; in two-photon spectroscopy, however, the overall outcome of absorbing two photons is a $g \rightarrow g$ or a $u \rightarrow u$ transition.

(b) Raman spectroscopy

Raman spectroscopy was revitalized by the introduction of lasers. An intense excitation beam increases the intensity of scattered radiation, so the use of laser sources increases the sensitivity of Raman spectroscopy. A well-defined beam also implies that the detector can be designed to collect only the radiation that has passed through a sample, and can be screened much more effectively against stray scattered light, which can obscure the Raman signal. The monochromaticity of laser radiation is also a great advantage, for it makes possible the observation of scattered light that differs by only fractions of reciprocal centimetres from the incident radiation. Such high resolution is particularly useful for observing the rotational structure of Raman lines because rotational transitions are of the order of a few reciprocal centimetres. Monochromaticity

also allows observations to be made very close to absorption frequencies, giving rise to the techniques of Fourier-transform Raman spectroscopy (Section 13.1) and resonance Raman spectroscopy (Section 13.16b).

The availability of nondivergent beams makes possible a qualitatively different kind of spectroscopy. The beam is so well-defined that it is possible to observe Raman transitions very close to the direction of propagation of the incident beam. This configuration is employed in the technique called **stimulated Raman spectroscopy**. In this form of spectroscopy, the Stokes and anti-Stokes radiation in the forward direction are powerful enough to undergo more scattering and hence give up or acquire more quanta of energy from the molecules in the sample. This multiple scattering results in lines of frequency $\nu_i \pm 2\nu_M$, $\nu_i \pm 3\nu_M$, and so on, where ν_i is the frequency of the incident radiation and ν_M the frequency of a molecular excitation.

(c) Precision-specified transitions

The monochromatic character of laser radiation is a very powerful characteristic because it allows us to excite specific states with very high precision. One consequence of state-specificity for photochemistry is that the illumination of a sample may be photochemically precise and hence efficient in stimulating a reaction, because its frequency can be tuned exactly to an absorption. The specific excitation of a particular excited state of a molecule may greatly enhance the rate of a reaction even at low temperatures. The rate of a reaction is generally increased by raising the temperature because the energies of the various modes of motion of the molecule are enhanced. However, this enhancement increases the energy of all the modes, even those that do not contribute appreciably to the reaction rate. With a laser we can excite the kinetically significant mode, so rate enhancement is achieved most efficiently. An example is the reaction

$$BCl_3 + C_6H_6 \rightarrow C_6H_5{-}BCl_2 + HCl$$

which normally proceeds only above 600°C in the presence of a catalyst; exposure to 10.6 μm CO_2 laser radiation results in the formation of products at room temperature without a catalyst. The commercial potential of this procedure is considerable (provided laser photons can be produced sufficiently cheaply), because heat-sensitive compounds, such as pharmaceuticals, may perhaps be made at lower temperatures than in conventional reactions.

A related application is the study of **state-to-state reaction dynamics**, in which a specific state of a reactant molecule is excited and we monitor not only the rate at which it forms products but also the states in which they are produced. Studies such as these give highly detailed information about the deployment of energy in chemical reactions (Chapter 24).

(d) Isotope separation

The precision state-selectivity of lasers is also of considerable potential for laser isotope separation. Isotope separation is possible because two **isotopomers**, or species that differ only in their isotopic composition, have slightly different energy levels and hence slightly different absorption frequencies.

One approach is to use **photoionization**, the ejection of an electron by the absorption of electromagnetic radiation. Direct photoionization by the absorption of a single photon does not distinguish between isotopomers because the upper level belongs to a continuum; to distinguish isotopomers it is necessary to deal with discrete states. At least two absorption processes are required. In the first step, a photon excites an atom to a higher state; in the second step, a photon achieves photoionization from that state (Fig. 14.35). The energy separation between the two states involved in the first step

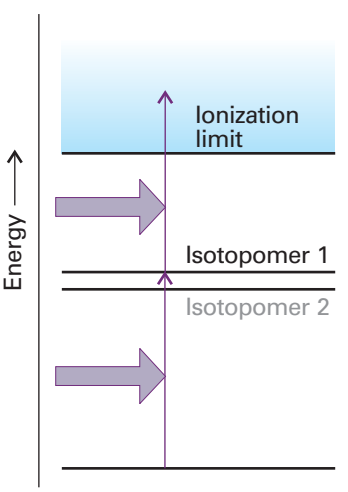

Fig. 14.35 In one method of isotope separation, one photon excites an isotopomer to an excited state, and then a second photon achieves photoionization. The success of the first step depends on the nuclear mass.

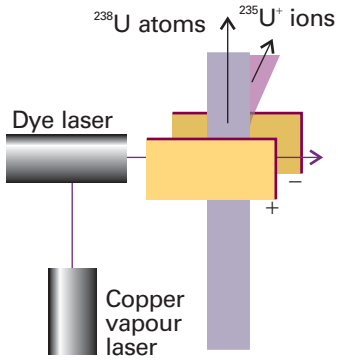

Fig. 14.36 An experimental arrangement for isotope separation. The dye laser, which is pumped by a copper-vapour laser, photoionizes the U atoms selectively according to their mass, and the ions are deflected by the electric field applied between the plates.

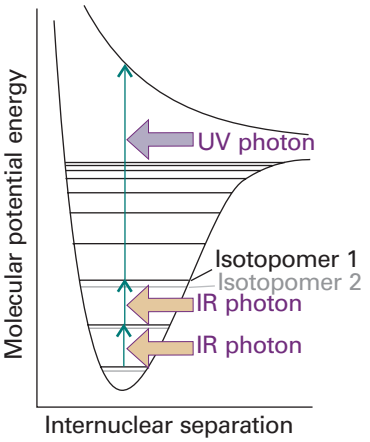

Fig. 14.37 Isotopomers may be separated by making use of their selective absorption of infrared photons followed by photodissociation with an ultraviolet photon.

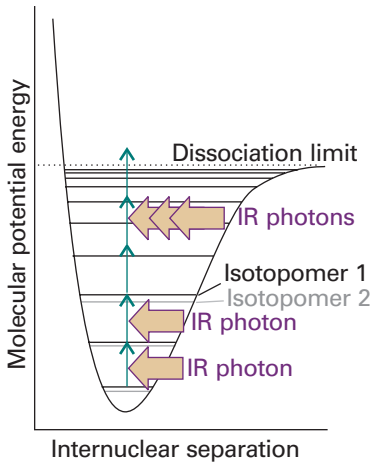

Fig. 14.38 In an alternative scheme for separating isotopomers, multiphoton absorption of infrared photons is used to reach the dissociation limit of a ground electronic state.

depends on the nuclear mass. Therefore, if the laser radiation is tuned to the appropriate frequency, only one of the isotopomers will undergo excitation and hence be available for photoionization in the second step. An example of this procedure is the photoionization of uranium vapour, in which the incident laser is tuned to excite ^{235}U but not ^{238}U. The ^{235}U atoms in the atomic beam are ionized in the two-step process; they are then attracted to a negatively charged electrode, and may be collected (Fig. 14.36). This procedure is being used in the latest generation of uranium separation plants.

Molecular isotopomers are used in techniques based on **photodissociation**, the fragmentation of a molecule following absorption of electromagnetic radiation. The key problem is to achieve both mass selectivity (which requires excitation to take place between discrete states) and dissociation (which requires excitation to continuum states). In one approach, two lasers are used: an infrared photon excites one isotopomer selectively to a higher vibrational level, and then an ultraviolet photon completes the process of photodissociation (Fig. 14.37). An alternative procedure is to make use of multiphoton absorption within the ground electronic state (Fig. 14.38); the efficiency of absorption of the first few photons depends on the match of their frequency to the energy level separations, so it is sensitive to nuclear mass. The absorbed photons open the door to a subsequent influx of enough photons to complete the dissociation process. The isotopomers $^{32}SF_6$ and $^{34}SF_6$ have been separated in this way.

In a third approach, a selectively vibrationally excited species may react with another species and give rise to products that can be separated chemically. This procedure has been employed successfully to separate isotopes of B, N, O, and, most efficiently, H. A variation on this procedure is to achieve selective **photoisomerization**, the conversion of a species to one of its isomers (particularly a geometrical isomer) on absorption of electromagnetic radiation. Once again, the initial absorption, which is isotope selective, opens the way to subsequent further absorption and the formation of a geometrical isomer that can be separated chemically. The approach has been used with the photoisomerization of CH_3NC to CH_3CN.

A different, more physical approach, that of **photodeflection**, is based on the recoil that occurs when a photon is absorbed by an atom and the linear momentum of the photon (which is equal to h/λ) is transferred to the atom. The atom is deflected from

its original path only if the absorption actually occurs, and the incident radiation can be tuned to a particular isotope. The deflection is very small, so an atom must absorb dozens of photons before its path is changed sufficiently to allow collection. For instance, if a Ba atom absorbs about 50 photons of 550 nm light, it will be deflected by only about 1 mm after a flight of 1 m.

(e) Time-resolved spectroscopy

The ability of lasers to produce pulses of very short duration is particularly useful in chemistry when we want to monitor processes in time. *Q*-switched lasers produce nanosecond pulses, which are generally fast enough to study reactions with rates controlled by the speed with which reactants can move through a fluid medium. However, when we want to study the rates at which energy is converted from one mode to another within a molecule, we need femtosecond and picosecond pulses. These timescales are available from mode-locked lasers.

In **time-resolved spectroscopy**, laser pulses are used to obtain the absorption, emission, or Raman spectrum of reactants, intermediates, products, and even transition states of reactions. It is also possible to study energy transfer, molecular rotations, vibrations, and conversion from one mode of motion to another. We shall see some of the information obtained from time-resolved spectroscopy in Chapters 22 to 24. Here, we describe some of the experimental techniques that employ pulsed lasers.

The arrangement shown in Fig. 14.39 is often used to study ultrafast chemical reactions that can be initiated by light, such as the initial events of vision (*Impact I14.1*). A strong and short laser pulse, the *pump*, promotes a molecule A to an excited electronic state A* that can either emit a photon (as fluorescence or phosphorescence) or react with another species B to yield a product C:

$$\begin{aligned} &A + h\nu \rightarrow A^* && \text{(absorption)}\\ &A^* \rightarrow A && \text{(emission)}\\ &A^* + B \rightarrow [AB] \rightarrow C && \text{(reaction)} \end{aligned}$$

Here [AB] denotes either an intermediate or an activated complex. The rates of appearance and disappearance of the various species are determined by observing time-dependent changes in the absorption spectrum of the sample during the course of the reaction. This monitoring is done by passing a weak pulse of white light, the *probe*, through the sample at different times after the laser pulse. Pulsed 'white' light can be generated directly from the laser pulse by the phenomenon of **continuum generation**, in which focusing an ultrafast laser pulse on a vessel containing a liquid such as water, carbon tetrachloride, CaF, or sapphire results in an outgoing beam with a wide distribution of frequencies. A time delay between the strong laser pulse and the 'white' light pulse can be introduced by allowing one of the beams to travel a longer distance before reaching the sample. For example, a difference in travel distance of $\Delta d = 3$ mm corresponds to a time delay $\Delta t = \Delta d/c \approx 10$ ps between two beams, where c is the speed of light. The relative distances travelled by the two beams in Fig. 14.39 are controlled by directing the 'white' light beam to a motorized stage carrying a pair of mirrors.

Variations of the arrangement in Fig. 14.39 allow for the observation of fluorescence decay kinetics of A* and time-resolved Raman spectra during the course of the reaction. The fluorescence lifetime of A* can be determined by exciting A as before and measuring the decay of the fluorescence intensity after the pulse with a fast photodetector system. In this case, continuum generation is not necessary. Time-resolved resonance Raman spectra of A, A*, B, [AB], or C can be obtained by initiating the reaction with a strong laser pulse of a certain wavelength and then, some time later, irradiating the sample with another laser pulse that can excite the resonance Raman

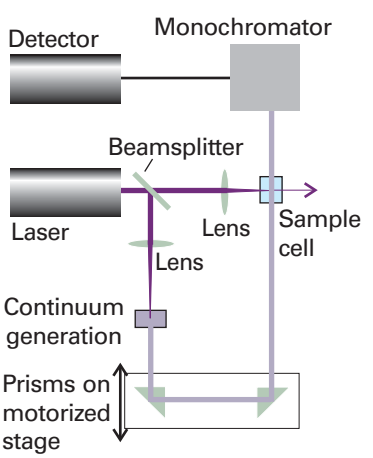

Fig. 14.39 A configuration used for time-resolved absorption spectroscopy, in which the same pulsed laser is used to generate a monochromatic pump pulse and, after continuum generation in a suitable liquid, a 'white' light probe pulse. The time delay between the pump and probe pulses may be varied by moving the motorized stage in the direction shown by the double arrow.

spectrum of the desired species. Also in this case continuum generation is not necessary. Instead, the Raman excitation beam may be generated in a dye laser (see *Further information 14.1*) or by stimulated Raman scattering of the laser pulse in a medium such as $H_2(g)$ or $CH_4(g)$.

(f) Spectroscopy of single molecules

There is great interest in the development of new experimental probes of very small specimens. On the one hand, our understanding of biochemical processes, such as enzymatic catalysis, protein folding, and the insertion of DNA into the cell's nucleus, will be enhanced if it is possible to visualize individual biopolymers at work. On the other hand, techniques that can probe the structure, dynamics, and reactivity of single molecules will be needed to advance research on nanometre-sized materials (*Impact I20.2*).

We saw in *Impact I13.3* that it is possible to obtain the vibrational spectrum of samples with areas of more than 10 μm^2. Fluorescence microscopy (*Impact I14.2*) has also been used for many years to image biological cells, but the diffraction limit prevents the visualization of samples that are smaller than the wavelength of light used as a probe (*Impact I13.3*). Most molecules—including biological polymers—have dimensions that are much smaller than visible wavelengths, so special techniques had to be developed to make single-molecule spectroscopy possible.

The bulk of the work done in the field of single-molecule spectroscopy is based on fluorescence microscopy with laser excitation. The laser is the radiation source of choice because it provides the high excitance required to increase the rate of arrival of photons on to the detector from small illuminated areas. Two techniques are commonly used to circumvent the diffraction limit. First, the concentration of the sample is kept so low that, on average, only one fluorescent molecule is in the illuminated area. Second, special strategies are used to illuminate very small volumes. In **near-field optical microscopy** (NSOM), a very thin metal-coated optical fibre is used to deliver light to a small area. It is possible to construct fibres with tip diameters in the range of 50 to 100 nm, which are indeed smaller than visible wavelengths. The fibre tip is placed very close to the sample, in a region known as the *near field*, where, according to classical physics, photons do not diffract. Figure 14.40 shows the image of a 4.5 μm × 4.5 μm sample of oxazine 720 dye molecules embedded in a polymer film and obtained with NSOM by measuring the fluorescence intensity as the tip is scanned over the film surface. Each peak corresponds to a single dye molecule.

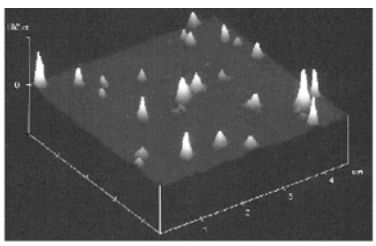

Fig. 14.40 Image of a 4.5 μm × 4.5 μm sample of oxazine-720 dye molecules embedded in a polymer film and obtained with NSOM. Each peak corresponds to a single dye molecule. Reproduced with permission from X.S. Xie. *Acc. Chem. Res.* 1996, **29**, 598.

In **far-field confocal microscopy**, laser light focused by an objective lens is used to illuminate about 1 μm^3 of a very dilute sample placed beyond the near field. This illumination scheme is limited by diffraction and, as a result, data from far-field microscopy have less structural detail than data from NSOM. However, far-field microscopes are very easy to construct and the technique can be used to probe single molecules as long as there is one molecule, on average, in the illuminated area.

In the **wide-field epifluorescence method**, a two-dimensional array detector (*Further information 13.1*) detects fluorescence excited by a laser and scattered scattered back from the sample (Fig. 14.41a). If the fluorescing molecules are well separated in the specimen, then it is possible to obtain a map of the distribution of fluorescent molecules in the illuminated area. For example, Fig. 14.41b shows how epifluorescence microscopy can be used to observe single molecules of the major histocompatibility (MHC) protein on the surface of a cell.

Though still a relatively new technique, single-molecule spectroscopy has already been used to address important problems in chemistry and biology. Nearly all the techniques discussed in this text measure the average value of a property in a large ensemble of molecules. Single-molecule methods allow a chemist to study the nature

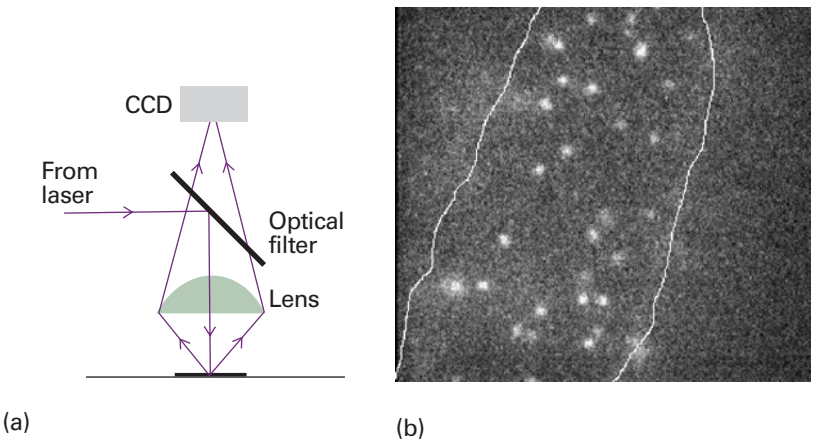

Fig. 14.41 (a) Layout of an epifluorescence microscope. Laser radiation is diverted to a sample by a special optical filter that reflects radiation with a specified wavelength (in this case the laser excitation wavelength) but transmits radiation with other wavelengths (in this case, wavelengths at which the fluorescent label emits). A CCD detector (see *Further information 13.1*) analyses the spatial distribution of the fluorescence signal from the illuminated area. (b) Observation of fluorescence from single MHC proteins that have been labelled with a fluorescent marker and are bound to the surface of a cell (the area shown has dimensions of 12 μm × 12 μm). Image provided by Professor W.E. Moerner, Stanford University, USA.

of distributions of physical and chemical properties in an ensemble of molecules. For example, it is possible to measure the fluorescence lifetime of a molecule by moving the laser focus to a location on the sample that contains a molecule and then measuring the decay of fluorescence intensity after excitation with a pulsed laser. Such studies have shown that not every molecule in a sample has the same fluorescence lifetime, probably because each molecule interacts with its immediate environment in a slightly different way. These details are not apparent from conventional measurements of fluorescence lifetimes, in which many molecules are excited electronically and only an average lifetime for the ensemble can be measured.

Checklist of key ideas

- ☐ 1. The selection rules for electronic transitions that are concerned with changes in angular momentum are: $\Delta\Lambda = 0, \pm1$, $\Delta S = 0$, $\Delta\Sigma = 0$, $\Delta\Omega = 0, \pm1$.
- ☐ 2. The Laporte selection rule (for centrosymmetric molecules) states that the only allowed transitions are transitions that are accompanied by a change of parity.
- ☐ 3. The Franck–Condon principle states that, because the nuclei are so much more massive than the electrons, an electronic transition takes place very much faster than the nuclei can respond.
- ☐ 4. The intensity of an electronic transition is proportional to the Franck–Condon factor, the quantity $|S(v_f,v_i)|^2$, with $S(v_f,v_i) = \langle v_f|v_i\rangle$.
- ☐ 5. Examples of electronic transitions include *d*–*d* transitions in *d*-metal complexes, charge-transfer transitions (a transition in which an electron moves from metal to ligand or from ligand to metal in a complex), $\pi^* \leftarrow \pi$, and $\pi^* \leftarrow n$ transitions.
- ☐ 6. A Jablonski diagram is a schematic diagram of the various types of nonradiative and radiative transitions that can occur in molecules.
- ☐ 7. Fluorescence is the spontaneous emission of radiation arising from a transition between states of the same multiplicity.
- ☐ 8. Phosphorescence is the spontaneous emission of radiation arising from a transition between states of different multiplicity.
- ☐ 9. Intersystem crossing is a nonradiative transition between states of different multiplicity.
- ☐ 10. Internal conversion is a nonradiative transition between states of the same multiplicity.
- ☐ 11. Laser action depends on the achievement of population inversion, an arrangement in which there are more molecules in an upper state than in a lower state, and the stimulated emission of radiation.
- ☐ 12. Resonant modes are the wavelengths that can be sustained by an optical cavity and contribute to the laser action. *Q*-switching is the modification of the resonance characteristics of the laser cavity and, consequently, of the laser output.
- ☐ 13. Mode locking is a technique for producing pulses of picosecond duration and less by matching the phases of many resonant cavity modes.
- ☐ 14. Applications of lasers in chemistry include multiphoton spectroscopy, Raman spectroscopy, precision-specified transitions, isotope separation, time-resolved spectroscopy, and single-molecule spectroscopy.

Further reading

Articles and texts

G. Herzberg, *Molecular spectra and molecular structure I. Spectra of diatomic molecules*. Krieger, Malabar (1989).

G. Herzberg, *Molecular spectra and molecular structure III. Electronic spectra and electronic structure of polyatomic molecules*. Van Nostrand–Reinhold, New York (1966).

J.R. Lakowicz, *Principles of fluorescence spectroscopy*. Kluwer/Plenum, New York (1999).

J.C. Lindon, G.E. Tranter, and J.L. Holmes (ed.), *Encyclopedia of spectroscopy and spectrometry*. Academic Press, San Diego (2000).

G.R. van Hecke and K.K. Karukstis, *A guide to lasers in chemistry*. Jones and Bartlett, Boston (1998).

G. Steinmeyer, D.H. Sutter, L. Gallmann, N. Matuschek, and U. Keller, Frontiers in ultrashort pulse generation: pushing the limits in linear and nonlinear optics. *Science* 1999, **286**, 1507.

Sources of data and information

M.E. Jacox, *Vibrational and electronic energy levels of polyatomic transient molecules*. Journal of Physical and Chemical Reference Data , Monograph No. 3 (1994).

D.R. Lide (ed.), *CRC Handbook of Chemistry and Physics*, Sections 9 and 10, CRC Press, Boca Raton (2000).

Further information

Further information 14.1 *Examples of practical lasers*

Figure 14.42 summarizes the requirements for an efficient laser. In practice, the requirements can be satisfied by using a variety of different systems, and this section reviews some that are commonly available. We also include some lasers that operate by using other than electronic transitions. Noticeably absent from this discussion are solid state lasers (including the ubiquitous diode lasers), which we discuss in Chapter 20.

Comment 14.3

The web site for this text contains links to databases on the optical properties of laser materials.

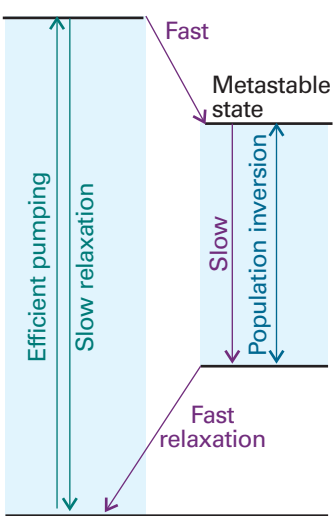

Fig. 14.42 A summary of the features needed for efficient laser action.

Gas lasers

Because gas lasers can be cooled by a rapid flow of the gas through the cavity, they can be used to generate high powers. The pumping is normally achieved using a gas that is different from the gas responsible for the laser emission itself.

In the **helium–neon laser** the active medium is a mixture of helium and neon in a mole ratio of about 5:1 (Fig. 14.43). The initial step is the excitation of an He atom to the metastable $1s^1 2s^1$

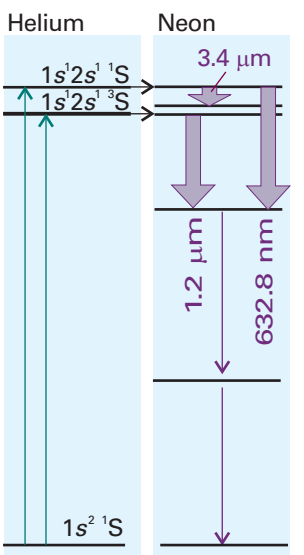

Fig. 14.43 The transitions involved in a helium–neon laser. The pumping (of the neon) depends on a coincidental matching of the helium and neon energy separations, so excited He atoms can transfer their excess energy to Ne atoms during a collision.

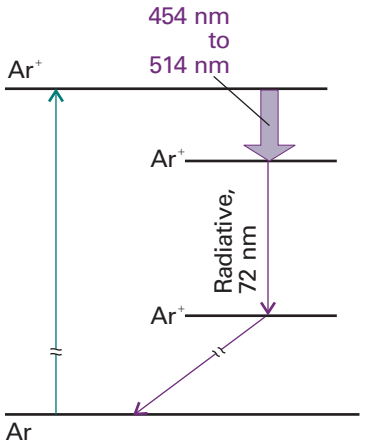

Fig. 14.44 The transitions involved in an argon-ion laser.

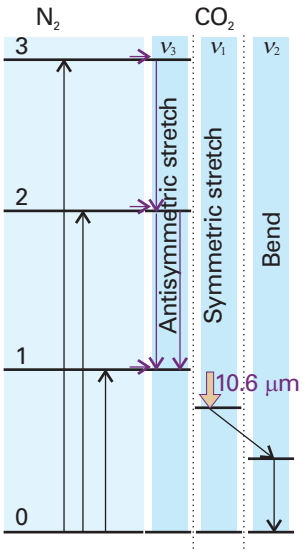

Fig. 14.45 The transitions involved in a carbon dioxide laser. The pumping also depends on the coincidental matching of energy separations; in this case the vibrationally excited N_2 molecules have excess energies that correspond to a vibrational excitation of the antisymmetric stretch of CO_2. The laser transition is from $\nu_3 = 1$ to $\nu_1 = 1$.

configuration by using an electric discharge (the collisions of electrons and ions cause transitions that are not restricted by electric-dipole selection rules). The excitation energy of this transition happens to match an excitation energy of neon, and during an He–Ne collision efficient transfer of energy may occur, leading to the production of highly excited, metastable Ne atoms with unpopulated intermediate states. Laser action generating 633 nm radiation (among about 100 other lines) then occurs.

The **argon-ion laser** (Fig.14.44), one of a number of 'ion lasers', consists of argon at about 1 Torr, through which is passed an electric discharge. The discharge results in the formation of Ar^+ and Ar^{2+} ions in excited states, which undergo a laser transition to a lower state. These ions then revert to their ground states by emitting hard ultraviolet radiation (at 72 nm), and are then neutralized by a series of electrodes in the laser cavity. One of the design problems is to find materials that can withstand this damaging residual radiation. There are many lines in the laser transition because the excited ions may make transitions to many lower states, but two strong emissions from Ar^+ are at 488 nm (blue) and 514 nm (green); other transitions occur elsewhere in the visible region, in the infrared, and in the ultraviolet. The **krypton-ion laser** works similarly. It is less efficient, but gives a wider range of wavelengths, the most intense being at 647 nm (red), but it can also generate yellow, green, and violet lines. Both lasers are widely used in laser light shows (for this application argon and krypton are often used simultaneously in the same cavity) as well as laboratory sources of high-power radiation.

The **carbon dioxide laser** works on a slightly different principle (Fig. 14.45), for its radiation (between 9.2 μm and 10.8 μm, with the strongest emission at 10.6 μm, in the infrared) arises from vibrational transitions. Most of the working gas is nitrogen, which becomes vibrationally excited by electronic and ionic collisions in an electric discharge. The vibrational levels happen to coincide with the ladder of antisymmetric stretch (ν_3, see Fig. 13.40) energy levels of CO_2, which pick up the energy during a collision. Laser action then occurs from the lowest excited level of ν_3 to the lowest excited level of the symmetric stretch (ν_1), which has remained unpopulated during the collisions. This transition is allowed by anharmonicities in the molecular potential energy. Some helium is included in the gas to help remove energy from this state and maintain the population inversion.

In a **nitrogen laser**, the efficiency of the stimulated transition (at 337 nm, in the ultraviolet, the transition $C^3\Pi_u \rightarrow B^3\Pi_g$) is so great that a single passage of a pulse of radiation is enough to generate laser radiation and mirrors are unnecessary: such lasers are said to be **superradiant**.

Chemical and exciplex lasers

Chemical reactions may also be used to generate molecules with nonequilibrium, inverted populations. For example, the photolysis of Cl_2 leads to the formation of Cl atoms which attack H_2 molecules in the mixture and produce HCl and H. The latter then attacks Cl_2 to produce vibrationally excited ('hot') HCl molecules. Because the newly formed HCl molecules have nonequilibrium vibrational populations, laser action can result as they return to lower states. Such processes are remarkable examples of the direct conversion of chemical energy into coherent electromagnetic radiation.

The population inversion needed for laser action is achieved in a more underhand way in **exciplex lasers**, for in these (as we shall see) the lower state does not effectively exist. This odd situation is achieved by forming an **exciplex**, a combination of two atoms that survives only in an excited state and which dissociates as soon as the excitation energy has been discarded. An exciplex can be formed in a mixture of xenon, chlorine, and neon (which acts as a buffer gas). An electric discharge through the mixture produces excited Cl atoms, which attach to the Xe atoms to give the exciplex XeCl*. The exciplex survives for about 10 ns, which is time for it to participate in laser action at 308 nm (in the ultraviolet). As soon as XeCl* has discarded a

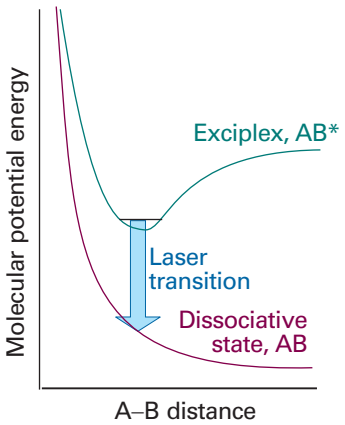

Fig. 14.46 The molecular potential energy curves for an exciplex. The species can survive only as an excited state, because on discarding its energy it enters the lower, dissociative state. Because only the upper state can exist, there is never any population in the lower state.

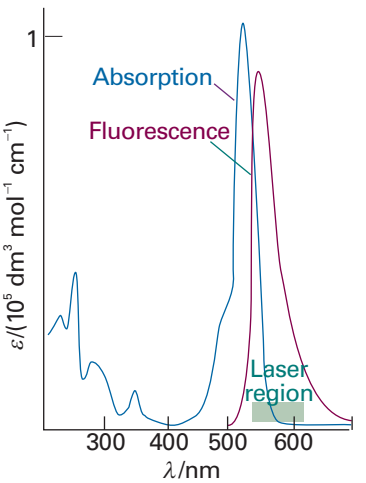

Fig. 14.47 The optical absorption spectrum of the dye Rhodamine 6G and the region used for laser action.

photon, the atoms separate because the molecular potential energy curve of the ground state is dissociative, and the ground state of the exciplex cannot become populated (Fig. 14.46). The KrF* exciplex laser is another example: it produces radiation at 249 nm.

Comment 14.4

The term 'excimer laser' is also widely encountered and used loosely when 'exciplex laser' is more appropriate. An exciplex has the form AB* whereas an excimer, an excited dimer, is AA*.

Dye lasers

Gas lasers and most solid state lasers operate at discrete frequencies and, although the frequency required may be selected by suitable optics, the laser cannot be tuned continuously. The tuning problem is overcome by using a titanium sapphire laser (see above) or a **dye laser**, which has broad spectral characteristics because the solvent broadens the vibrational structure of the transitions into bands. Hence, it is possible to scan the wavelength continuously (by rotating the diffraction grating in the cavity) and achieve laser action at any chosen wavelength. A commonly used dye is rhodamine 6G in methanol (Fig. 14.47). As the gain is very high, only a short length of the optical path need be through the dye. The excited states of the active medium, the dye, are sustained by another laser or a flash lamp, and the dye solution is flowed through the laser cavity to avoid thermal degradation (Fig. 14.48).

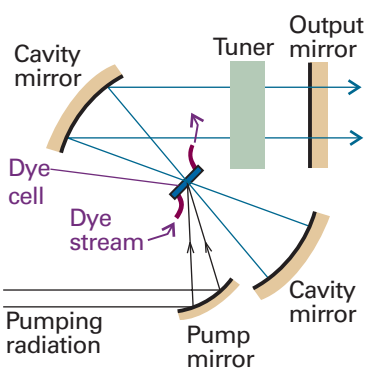

Fig. 14.48 The configuration used for a dye laser. The dye is flowed through the cell inside the laser cavity. The flow helps to keep it cool and prevents degradation.

Discussion questions

14.1 Explain the origin of the term symbol $^3\Sigma_g^-$ for the ground state of dioxygen.

14.2 Explain the basis of the Franck–Condon principle and how it leads to the formation of a vibrational progression.

14.3 How do the band heads in P and R branches arise? Could the Q branch show a head?

14.4 Explain how colour can arise from molecules.

14.5 Describe the mechanism of fluorescence. To what extent is a fluorescence spectrum not the exact mirror image of the corresponding absorption spectrum?

14.6 What is the evidence for the correctness of the mechanism of fluorescence?

14.7 Describe the principles of laser action, with actual examples.

14.8 What features of laser radiation are applied in chemistry? Discuss two applications of lasers in chemistry.

Exercises

14.1a The term symbol for the ground state of N_2^+ is $^2\Sigma_g^+$. What is the total spin and total orbital angular momentum of the molecule? Show that the term symbol agrees with the electron configuration that would be predicted using the building-up principle.

14.1b One of the excited states of the C_2 molecule has the valence electron configuration $1\sigma_g^2 1\sigma_u^2 1\pi_u^3 1\pi_g^1$. Give the multiplicity and parity of the term.

14.2a The molar absorption coefficient of a substance dissolved in hexane is known to be 855 $dm^3\ mol^{-1}\ cm^{-1}$ at 270 nm. Calculate the percentage reduction in intensity when light of that wavelength passes through 2.5 mm of a solution of concentration 3.25 mmol dm^{-3}.

14.2b The molar absorption coefficient of a substance dissolved in hexane is known to be 327 $dm^3\ mol^{-1}\ cm^{-1}$ at 300 nm. Calculate the percentage reduction in intensity when light of that wavelength passes through 1.50 mm of a solution of concentration 2.22 mmol dm^{-3}.

14.3a A solution of an unknown component of a biological sample when placed in an absorption cell of path length 1.00 cm transmits 20.1 per cent of light of 340 nm incident upon it. If the concentration of the component is 0.111 mmol dm^{-3}, what is the molar absorption coefficient?

14.3b When light of wavelength 400 nm passes through 3.5 mm of a solution of an absorbing substance at a concentration 0.667 mmol dm^{-3}, the transmission is 65.5 per cent. Calculate the molar absorption coefficient of the solute at this wavelength and express the answer in $cm^2\ mol^{-1}$.

14.4a The molar absorption coefficient of a solute at 540 nm is 286 $dm^3\ mol^{-1}\ cm^{-1}$. When light of that wavelength passes through a 6.5 mm cell containing a solution of the solute, 46.5 per cent of the light is absorbed. What is the concentration of the solution?

14.4b The molar absorption coefficient of a solute at 440 nm is 323 $dm^3\ mol^{-1}\ cm^{-1}$. When light of that wavelength passes through a 7.50 mm cell containing a solution of the solute, 52.3 per cent of the light is absorbed. What is the concentration of the solution?

14.5a The absorption associated with a particular transition begins at 230 nm, peaks sharply at 260 nm, and ends at 290 nm. The maximum value of the molar absorption coefficient is 1.21×10^4 $dm^3\ mol^{-1}\ cm^{-1}$. Estimate the integrated absorption coefficient of the transition assuming a triangular lineshape (see eqn 13.5).

14.5b The absorption associated with a certain transition begins at 199 nm, peaks sharply at 220 nm, and ends at 275 nm. The maximum value of the molar absorption coefficient is 2.25×10^4 $dm^3\ mol^{-1}\ cm^{-1}$. Estimate the integrated absorption coefficient of the transition assuming an inverted parabolic lineshape (Fig. 14.49; use eqn 13.5).

14.6a The two compounds, 2,3-dimethyl-2-butene and 2,5-dimethyl-2,4-hexadiene, are to be distinguished by their ultraviolet absorption spectra. The maximum absorption in one compound occurs at 192 nm and in the other at 243 nm. Match the maxima to the compounds and justify the assignment.

14.6b 1,3,5-hexatriene (a kind of 'linear' benzene) was converted into benzene itself. On the basis of a free-electron molecular orbital model (in which hexatriene is treated as a linear box and benzene as a ring), would you expect the lowest energy absorption to rise or fall in energy?

14.7a The following data were obtained for the absorption by Br_2 in carbon tetrachloride using a 2.0 mm cell. Calculate the molar absorption coefficient of bromine at the wavelength employed:

$[Br_2]/(mol\ dm^{-3})$	0.0010	0.0050	0.0100	0.0500
T/(per cent)	81.4	35.6	12.7	3.0×10^{-3}

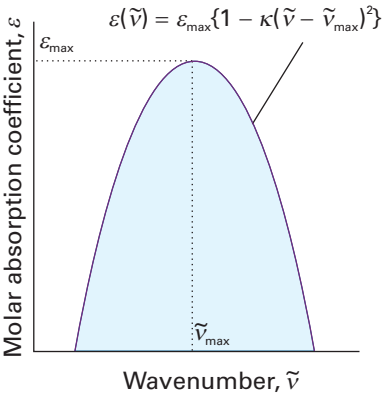

Fig. 14.49

14.7b The following data were obtained for the absorption by a dye dissolved in methylbenzene using a 2.50 mm cell. Calculate the molar absorption coefficient of the dye at the wavelength employed:

[dye]/(mol dm^{-3})	0.0010	0.0050	0.0100	0.0500
T/(per cent)	73	21	4.2	1.33×10^{-5}

14.8a A 2.0-mm cell was filled with a solution of benzene in a non-absorbing solvent. The concentration of the benzene was 0.010 mol dm^{-3} and the wavelength of the radiation was 256 nm (where there is a maximum in the absorption). Calculate the molar absorption coefficient of benzene at this wavelength given that the transmission was 48 per cent. What will the transmittance be in a 4.0-mm cell at the same wavelength?

14.8b A 2.50-mm cell was filled with a solution of a dye. The concentration of the dye was 15.5 mmol dm^{-3}. Calculate the molar absorption coefficient of benzene at this wavelength given that the transmission was 32 per cent. What will the transmittance be in a 4.50-mm cell at the same wavelength?

14.9a A swimmer enters a gloomier world (in one sense) on diving to greater depths. Given that the mean molar absorption coefficient of sea water in the visible region is 6.2×10^{-3} $dm^3\ mol^{-1}\ cm^{-1}$, calculate the depth at which a diver will experience (a) half the surface intensity of light, (b) one tenth the surface intensity.

14.9b Given that the maximum molar absorption coefficient of a molecule containing a carbonyl group is 30 $dm^3\ mol^{-1}\ cm^{-1}$ near 280 nm, calculate the thickness of a sample that will result in (a) half the initial intensity of radiation, (b) one-tenth the initial intensity.

14.10a The electronic absorption bands of many molecules in solution have half-widths at half-height of about 5000 cm^{-1}. Estimate the integrated absorption coefficients of bands for which (a) $\varepsilon_{max} \approx 1 \times 10^4$ $dm^3\ mol^{-1}\ cm^{-1}$, (b) $\varepsilon_{max} \approx 5 \times 10^2$ $dm^3\ mol^{-1}\ cm^{-1}$.

14.10b The electronic absorption band of a compound in solution had a Gaussian lineshape and a half-width at half-height of 4233 cm^{-1} and $\varepsilon_{max} = 1.54 \times 10^4$ $dm^3\ mol^{-1}\ cm^{-1}$. Estimate the integrated absorption coefficient.

14.11a The photoionization of H_2 by 21 eV photons produces H_2^+. Explain why the intensity of the $v = 2 \leftarrow 0$ transition is stronger than that of the $0 \leftarrow 0$ transition.

14.11b The photoionization of F_2 by 21 eV photons produces F_2^+. Would you expect the $2 \leftarrow 0$ transition to be weaker or stronger than the $0 \leftarrow 0$ transition? Justify your answer.

Problems*

Numerical problems

14.1 The vibrational wavenumber of the oxygen molecule in its electronic ground state is 1580 cm^{-1}, whereas that in the first excited state ($B\ ^3\Sigma_u^-$), to which there is an allowed electronic transition, is 700 cm^{-1}. Given that the separation in energy between the minima in their respective potential energy curves of these two electronic states is 6.175 eV, what is the wavenumber of the lowest energy transition in the band of transitions originating from the $v = 0$ vibrational state of the electronic ground state to this excited state? Ignore any rotational structure or anharmonicity.

14.2 A Birge–Sponer extrapolation yields 7760 cm^{-1} as the area under the curve for the B state of the oxygen molecule described in Problem 14.1. Given that the B state dissociates to ground-state atoms (at zero energy, ^3P) and 15 870 cm^{-1} (^1D) and the lowest vibrational state of the B state is 49 363 cm^{-1} above the lowest vibrational state of the ground electronic state, calculate the dissociation energy of the molecular ground state to the ground-state atoms.

14.3 The electronic spectrum of the IBr molecule shows two low-lying, well defined convergence limits at 14 660 and 18 345 cm^{-1}. Energy levels for the iodine and bromine atoms occur at 0, 7598; and 0, 3685 cm^{-1}, respectively. Other atomic levels are at much higher energies. What possibilities exist for the numerical value of the dissociation energy of IBr? Decide which is the correct possibility by calculating this quantity from $\Delta_f H^\ominus$(IBr, g) = +40.79 kJ mol^{-1} and the dissociation energies of I_2(g) and Br_2(g) which are 146 and 190 kJ mol^{-1}, respectively.

14.4 In many cases it is possible to assume that an absorption band has a Gaussian lineshape (one proportional to e^{-x^2}) centred on the band maximum. Assume such a line shape, and show that $A \approx 1.0645\varepsilon_{max}\Delta\tilde{\nu}_{1/2}$, where $\Delta\tilde{\nu}_{1/2}$ is the width at half-height. The absorption spectrum of azoethane ($CH_3CH_2N_2$) between 24 000 cm^{-1} and 34 000 cm^{-1} is shown in Fig. 14.50. First, estimate A for the band by assuming that it is Gaussian. Then integrate the absorption band graphically. The latter can be done either by ruling and counting squares, or by tracing the lineshape on to paper and weighing. A more sophisticated procedure would be to use mathematical software to fit a polynomial to the absorption band (or a Gaussian), and then to integrate the result analytically.

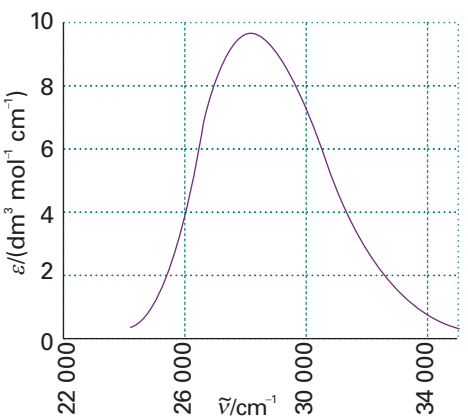

Fig. 14.50

14.5 A lot of information about the energy levels and wavefunctions of small inorganic molecules can be obtained from their ultraviolet spectra. An example of a spectrum with considerable vibrational structure, that of gaseous SO_2 at 25°C, is shown in Fig. 14.6. Estimate the integrated absorption coefficient for the transition. transition. What electronic states are accessible from the A_1 ground state of this C_v molecule by electric dipole transitions?

14.6‡ J.G. Dojahn, E.C.M. Chen, and W.E. Wentworth (*J. Phys. Chem.* **100**, 9649 (1996)) characterized the potential energy curves of the ground and electronic states of homonuclear diatomic halogen anions. These anions have a $^2\Sigma_u^+$ ground state and $^2\Pi_g$, $^2\Pi_u$, and $^2\Sigma_g^+$ excited states. To which of the excited states are transitions by absorption of photons allowed? Explain.

14.7 A transition of particular importance in O_2 gives rise to the 'Schumann–Runge band' in the ultraviolet region. The wavenumbers (in cm^{-1}) of transitions from the ground state to the vibrational levels of the first excited state ($^3\Sigma_u^-$) are 50 062.6, 50 725.4, 51 369.0, 51 988.6, 52 579.0, 53 143.4, 53 679.6, 54 177.0, 54 641.8, 55 078.2, 55 460.0, 55 803.1, 56 107.3, 56 360.3, 56 570.6. What is the dissociation energy of the upper electronic state? (Use a Birge–Sponer plot.) The same excited state is known to dissociate into one ground-state O atom and one excited-state atom with an energy 190 kJ mol^{-1} above the ground state. (This excited atom is responsible for a great deal of photochemical mischief in the atmosphere.) Ground-state O_2 dissociates into two ground-state atoms. Use this information to calculate the dissociation energy of ground-state O_2 from the Schumann–Runge data.

14.8 The compound $CH_3CH{=}CHCHO$ has a strong absorption in the ultraviolet at 46 950 cm^{-1} and a weak absorption at 30 000 cm^{-1}. Justify these features in terms of the structure of the molecule.

14.9 Aromatic hydrocarbons and I_2 form complexes from which charge-transfer electronic transitions are observed. The hydrocarbon acts as an electron donor and I_2 as an electron acceptor. The energies $h\nu_{max}$ of the charge-transfer transitions for a number of hydrocarbon–I_2 complexes are given below:

Hydrocarbon	benzene	biphenyl	naphthalene	phenanthrene	pyrene	anthracene
$h\nu_{max}$/eV	4.184	3.654	3.452	3.288	2.989	2.890

Investigate the hypothesis that there is a correlation between the energy of the HOMO of the hydrocarbon (from which the electron comes in the charge–transfer transition) and $h\nu_{max}$. Use one of the molecular electronic structure methods discussed in Chapter 11 to determine the energy of the HOMO of each hydrocarbon in the data set.[1]

14.10 A certain molecule fluoresces at a wavelength of 400 nm with a half-life of 1.0 ns. It phosphoresces at 500 nm. If the ratio of the transition probabilities for stimulated emission for the $S^* \rightarrow S$ to the $T \rightarrow S$ transitions is 1.0×10^5, what is the half-life of the phosphorescent state?

14.11 Consider some of the precautions that must be taken when conducting single-molecule spectroscopy experiments. (a) What is the molar concentration of a solution in which there is, on average, one solute molecule in 1.0 μm^3 (1.0 fL) of solution? (b) It is important to use pure solvents in single-molecule spectroscopy because optical signals from fluorescent

* Problems denoted with the symbol ‡ were supplied by Charles Trapp and Carmen Giunta.

[1] The web site contains links to molecular modelling freeware and to other sites where you may perform molecular orbital calculations directly from your web browser.

impurities in the solvent may mask optical signals from the solute. Suppose that water containing a fluorescent impurity of molar mass 100 g mol^{-1} is used as solvent and that analysis indicates the presence of 0.10 mg of impurity per 1.0 kg of solvent. On average, how many impurity molecules will be present in 1.0 μm^3 of solution? You may take the density of water as 1.0 g cm^{-3}. Comment on the suitability of this solvent for single-molecule spectroscopy experiments.

14.12 Light-induced degradation of molecules, also called *photobleaching*, is a serious problem in single-molecule spectroscopy. A molecule of a fluorescent dye commonly used to label biopolymers can withstand about 10^6 excitations by photons before light-induced reactions destroy its π system and the molecule no longer fluoresces. For how long will a single dye molecule fluoresce while being excited by 1.0 mW of 488 nm radiation from a continuous-wave argon ion laser? You may assume that the dye has an absorption spectrum that peaks at 488 nm and that every photon delivered by the laser is absorbed by the molecule.

Theoretical problems

14.13 Assume that the electronic states of the π electrons of a conjugated molecule can be approximated by the wavefunctions of a particle in a one-dimensional box, and that the dipole moment can be related to the displacement along this length by $\mu = -ex$. Show that the transition probability for the transition $n = 1 \rightarrow n = 2$ is nonzero, whereas that for $n = 1 \rightarrow n = 3$ is zero. *Hint*. The following relations will be useful:

$$\sin x \sin y = \tfrac{1}{2}\cos(x-y) - \tfrac{1}{2}\cos(x+y)$$

$$\int x \cos ax \, dx = \frac{1}{a^2}\cos ax + \frac{x}{a}\sin ax$$

14.14 Use a group theoretical argument to decide which of the following transitions are electric-dipole allowed: (a) the $\pi^* \leftarrow \pi$ transition in ethene, (b) the $\pi^* \leftarrow n$ transition in a carbonyl group in a C_{2v} environment.

14.15 Suppose that you are a colour chemist and had been asked to intensify the colour of a dye without changing the type of compound, and that the dye in question was a polyene. Would you choose to lengthen or to shorten the chain? Would the modification to the length shift the apparent colour of the dye towards the red or the blue?

14.16 One measure of the intensity of a transition of frequency ν is the *oscillator strength*, f, which is defined as

$$f = \frac{8\pi^2 m_e \nu |\boldsymbol{\mu}_{fi}|^2}{3he^2}$$

Consider an electron in an atom to be oscillating harmonically in one dimension (the three-dimensional version of this model was used in early attempts to describe atomic structure). The wavefunctions for such an electron are those in Table 9.1. Show that the oscillator strength for the transition of this electron from its ground state is exactly $\frac{1}{3}$.

14.17 Estimate the oscillator strength (see Problem 14.16) of a charge-transfer transition modelled as the migration of an electron from an H1s orbital on one atom to another H1s orbital on an atom a distance R away. Approximate the transition moment by $-eRS$ where S is the overlap integral of the two orbitals. Sketch the oscillator strength as a function of R using the curve for S given in Fig. 11.29. Why does the intensity fall to zero as R approaches 0 and infinity?

14.18 The line marked A in Fig. 14.51 is the fluorescence spectrum of benzophenone in solid solution in ethanol at low temperatures observed when the sample is illuminated with 360 nm light. What can be said about the vibrational energy levels of the carbonyl group in (a) its ground electronic state and (b) its excited electronic state? When naphthalene is illuminated with 360 nm light it does not absorb, but the line marked B in the illustration is the phosphorescence spectrum of a solid solution of a mixture of naphthalene and benzophenone in ethanol. Now a component of fluorescence from naphthalene can be detected. Account for this observation.

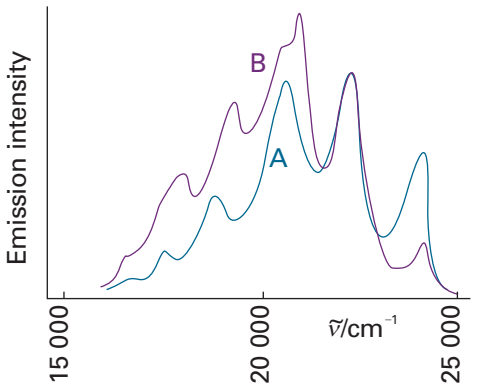

Fig. 14.51

14.19 The fluorescence spectrum of anthracene vapour shows a series of peaks of increasing intensity with individual maxima at 440 nm, 410 nm, 390 nm, and 370 nm followed by a sharp cut-off at shorter wavelengths. The absorption spectrum rises sharply from zero to a maximum at 360 nm with a trail of peaks of lessening intensity at 345 nm, 330 nm, and 305 nm. Account for these observations.

14.20 The Beer–Lambert law states that the absorbance of a sample at a wavenumber $\tilde{\nu}$ is proportional to the molar concentration [J] of the absorbing species J and to the length l of the sample (eqn 13.4). In this problem you will show that the intensity of fluorescence emission from a sample of J is also proportional to [J] and l. Consider a sample of J that is illuminated with a beam of intensity $I_0(\tilde{\nu})$ at the wavenumber $\tilde{\nu}$. Before fluorescence can occur, a fraction of $I_0(\tilde{\nu})$ must be absorbed and an intensity $I(\tilde{\nu})$ will be transmitted. However, not all of the absorbed intensity is emitted and the intensity of fluorescence depends on the fluorescence quantum yield, ϕ_f, the efficiency of photon emission. The fluorescence quantum yield ranges from 0 to 1 and is proportional to the ratio of the integral of the fluorescence spectrum over the integrated absorption coefficient. Because of a Stokes shift of magnitude $\Delta\tilde{\nu}_{Stokes}$, fluorescence occurs at a wavenumber $\tilde{\nu}_f$, with $\tilde{\nu}_f + \Delta\tilde{\nu}_{Stokes} = \tilde{\nu}$. It follows that the fluorescence intensity at $\tilde{\nu}_f$, $I_f(\tilde{\nu}_f)$, is proportional to ϕ_f and to the intensity of exciting radiation that is absorbed by J, $I_{abs}(\tilde{\nu}) = I_0(\tilde{\nu}) - I(\tilde{\nu})$. (a) Use the Beer–Lambert law to express $I_{abs}(\tilde{\nu})$ in terms of $I_0(\tilde{\nu})$, [J], l, and $\varepsilon(\tilde{\nu})$, the molar absorption coefficient of J at $\tilde{\nu}$. (b) Use your result from part (a) to show that $I_f(\tilde{\nu}_f) \propto I_0(\tilde{\nu})\varepsilon(\tilde{\nu})\phi_f[J]l$.

14.21 Spin angular momentum is conserved when a molecule dissociates into atoms. What atom multiplicities are permitted when (a) an O_2 molecule, (b) an N_2 molecule dissociates into atoms?

Applications: to biochemistry, environmental science, and astrophysics

14.22 The protein haemerythrin (Her) is responsible for binding and carrying O_2 in some invertebrates. Each protein molecule has two Fe^{2+} ions that are in very close proximity and work together to bind one molecule of O_2. The Fe_2O_2 group of oxygenated haemerythrin is coloured and has an electronic absorption band at 500 nm. Figure 14.52 shows the UV-visible absorption spectrum of a derivative of haemerythrin in the presence of different concentrations of CNS^- ions. What may be inferred from the spectrum?

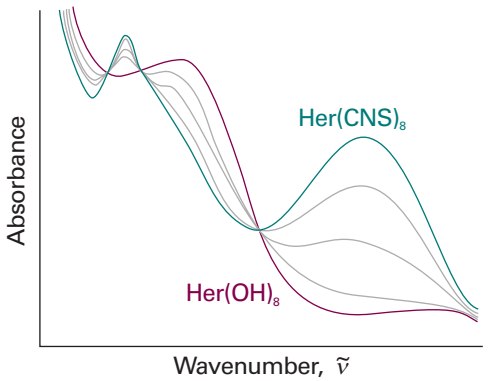

Fig. 14.52

14.23 The flux of visible photons reaching Earth from the North Star is about 4×10^3 mm^{-2} s^{-1}. Of these photons, 30 per cent are absorbed or scattered by the atmosphere and 25 per cent of the surviving photons are scattered by the surface of the cornea of the eye. A further 9 per cent are absorbed inside the cornea. The area of the pupil at night is about 40 mm^2 and the response time of the eye is about 0.1 s. Of the photons passing through the pupil, about 43 per cent are absorbed in the ocular medium. How many photons from the North Star are focused on to the retina in 0.1 s? For a continuation of this story, see R.W. Rodieck, *The first steps in seeing*, Sinauer, Sunderland (1998).

14.24 Use molecule (**7**) as a model of the *trans* conformation of the chromophore found in rhodopsin. In this model, the methyl group bound to the nitrogen atom of the protonated Schiff's base replaces the protein. (a) Using molecular modelling software and the computational method of your instructor's choice, calculate the energy separation between the HOMO and LUMO of (**7**). (b) Repeat the calculation for the 11-*cis* form of (**7**). (c) Based on your results from parts (a) and (b), do you expect the experimental frequency for the $\pi^* \leftarrow \pi$ visible absorption of the *trans* form of (**7**) to be higher or lower than that for the 11-*cis* form of (**7**)?

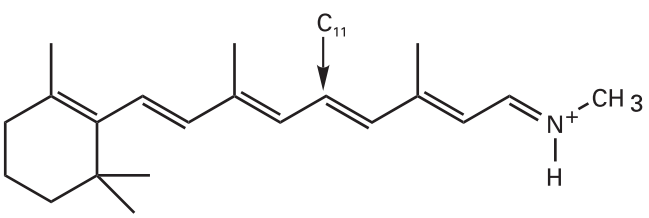

7

14.25‡ Ozone absorbs ultraviolet radiation in a part of the electromagnetic spectrum energetic enough to disrupt DNA in biological organisms and that is absorbed by no other abundant atmospheric constituent. This spectral range, denoted UV-B, spans the wavelengths of about 290 nm to 320 nm. The molar extinction coefficient of ozone over this range is given in the table below (W.B. DeMore, S.P. Sander, D.M. Golden, R.F. Hampson, M.J. Kurylo, C.J. Howard, A.R. Ravishankara, C.E. Kolb, and M.J. Molina, *Chemical kinetics and photochemical data for use in stratospheric modeling: Evaluation Number 11*, JPL Publication 94–26 (1994).

λ/nm	292.0	296.3	300.8	305.4	310.1	315.0	320.0
ε/(dm^3 mol^{-1} cm^{-1})	1512	865	477	257	135.9	69.5	34.5

Compute the integrated absorption coefficient of ozone over the wavelength range 290–320 nm. (*Hint*. $\varepsilon(\tilde{\nu})$ can be fitted to an exponential function quite well.)

14.26‡ The abundance of ozone is typically inferred from measurements of UV absorption and is often expressed in terms of *Dobson units* (DU): 1 DU is equivalent to a layer of pure ozone 10^{-3} cm thick at 1 atm and 0°C. Compute the absorbance of UV radiation at 300 nm expected for an ozone abundance of 300 DU (a typical value) and 100 DU (a value reached during seasonal Antarctic ozone depletions) given a molar absorption coefficient of 476 dm^3 mol^{-1} cm^{-1}.

14.27‡ G.C.G. Wachewsky, R. Horansky, and V. Vaida (*J. Phys. Chem.* **100**, 11559 (1996)) examined the UV absorption spectrum of CH_3I, a species of interest in connection with stratospheric ozone chemistry. They found the integrated absorption coefficient to be dependent on temperature and pressure to an extent inconsistent with internal structural changes in isolated CH_3I molecules; they explained the changes as due to dimerization of a substantial fraction of the CH_3I, a process that would naturally be pressure and temperature dependent. (a) Compute the integrated absorption coefficient over a triangular lineshape in the range 31 250 to 34 483 cm^{-1} and a maximal molar absorption coefficient of 150 dm^3 mol^{-1} cm^{-1} at 31 250 cm^{-1}. (b) Suppose 1 per cent of the CH_3I units in a sample at 2.4 Torr and 373 K exists as dimers. Compute the absorbance expected at 31 250 cm^{-1} in a sample cell of length 12.0 cm. (c) Suppose 18 per cent of the CH_3I units in a sample at 100 Torr and 373 K exists as dimers. Compute the absorbance expected at 31 250 cm^{-1} in a sample cell of length 12.0 cm; compute the molar absorption coefficient that would be inferred from this absorbance if dimerization was not considered.

14.28‡ The molecule Cl_2O_2 is believed to participate in the seasonal depletion of ozone over Antarctica. M. Schwell, H.-W. Jochims, B. Wassermann, U. Rockland, R. Flesch, and E. Rühl (*J. Phys. Chem.* **100**, 10070 (1996)) measured the ionization energies of Cl_2O_2 by photoelectron spectroscopy in which the ionized fragments were detected using a mass spectrometer. From their data, we can infer that the ionization enthalpy of Cl_2O_2 is 11.05 eV and the enthalpy of the dissociative ionization $Cl_2O_2 \rightarrow Cl + OClO^+ + e^-$ is 10.95 eV. They used this information to make some inferences about the structure of Cl_2O_2. Computational studies had suggested that the lowest energy isomer is ClOOCl, but that $ClClO_2$ (C_{2v}) and ClOClO are not very much higher in energy. The Cl_2O_2 in the photoionization step is the lowest energy isomer, whatever its structure may be, and its enthalpy of formation had previously been reported as +133 kJ mol^{-1}. The Cl_2O_2 in the dissociative ionization step is unlikely to be ClOOCl, for the product can be derived from it only with substantial rearrangement. Given $\Delta_f H^\ominus(OClO^+) = +1096$ kJ mol^{-1} and $\Delta_f H^\ominus(e^-) = 0$, determine whether the Cl_2O_2 in the dissociative ionization is the same as that in the photoionization. If different, how much greater is its $\Delta_f H^\ominus$? Are these results consistent with or contradictory to the computational studies?

14.29‡ One of the principal methods for obtaining the electronic spectra of unstable radicals is to study the spectra of comets, which are almost entirely due to radicals. Many radical spectra have been found in comets, including that due to CN. These radicals are produced in comets by the absorption of far ultraviolet solar radiation by their parent compounds. Subsequently, their fluorescence is excited by sunlight of longer wavelength. The spectra of comet Hale–Bopp (C/1995 O1) have been the subject of many recent studies. One such study is that of the fluorescence spectrum of CN in the comet at large heliocentric distances by R.M. Wagner and D.G. Schleicher (*Science* **275**, 1918 (1997)), in which the authors determine the spatial distribution and rate of production of CN in the coma. The (0–0) vibrational band is centred on 387.6 nm and the weaker (1–1) band with relative intensity 0.1 is centred on 386.4 nm. The band heads for (0–0) and (0–1) are known to be 388.3 and 421.6 nm, respectively. From these data, calculate the energy of the excited S_1 state relative to the ground S_0 state, the vibrational wavenumbers and the difference in the vibrational wavenumbers of the two states, and the relative populations of the $v = 0$ and $v = 1$ vibrational levels of the S_1 state. Also estimate the effective temperature of the molecule in the excited S_1 state. Only eight rotational levels of the S_1 state are thought to be populated. Is that observation consistent with the effective temperature of the S_1 state?